

Thermodynamics and Optical Conductivity of a Dissipative Carrier in a Tight Binding Model *

Takeo Kato and Masatoshi Imada

*Institute for Solid State Physics, University of Tokyo,
7-22-1 Roppongi, Minato-ku, Tokyo 106*

(Received December 2, 2024)

Thermodynamics and transport properties of a dissipative particle in a tight-binding model are studied through specific heat, optical conductivity and one-particle Green's functions. A weak coupling theory is constituted to study the crossover behavior between the low-temperature region and the high-temperature region analytically. For ohmic damping, the specific heat shows an unusual T -linear behavior at low temperatures, and the one-particle Green's function is local in space. This indicates that the environment strongly influences the particle motion, and makes it 'incoherent' in the sense that eigenstates of momenta are not good eigenstates to describe the low-energy states in the dissipative particle. For the ohmic damping, the optical conductivity $\sigma(\omega)$ takes the non-Drude form even at zero temperature, and the high-frequency side behaves as ω^{2K-2} , where K is the dimensionless damping strength. The high frequency side of the optical conductivity is independent of temperatures, while the low frequency side depends on the temperature, and behaves as T^{2K-2} at high temperatures.

KEYWORDS: dissipation, specific heat, optical conductivity, one-particle Green's function, ohmic damping, Kubo formula, coherence, incoherence

§1. Introduction

Quantum transport of a particle coupled to a heat bath has been studied for several decades in many areas of physics.¹⁾ For example, transport properties of a particle coupled to phonons have been studied in terms of polaron effects, while heavy particles such as muons coupled to the conduction electrons have been studied both theoretically^{2,3,4)} and experimentally.^{5,6)} In the latter case, heavy particles in metals move under a frequency-independent (ohmic) damping caused by conduction electrons. This problem is related to the Kondo problem⁷⁾ and the X-ray absorption edge anomaly.⁸⁾ The ohmic damping also controls dynamics of macroscopic variable such as phase difference of superconductors in Josephson devices,¹¹⁾ and in a quantum dot coupled to an additional quantum point contact.¹²⁾ Recently, it has been claimed that the ohmic damping is relevant to c -axis transport in high- T_c superconductors.^{9,10)}

From a theoretical point of view, a particle coupled to a heat bath has been studied mainly on a basis of a phenomenological model by Caldeira and Leggett.¹³⁾ This model has offered many applications such as decay of a metastable state,¹³⁾ motion in a double well¹⁴⁾ or a periodic potential,^{15,16,17,18)} and the Brownian motion.¹⁹⁾ Generally, it is proved that damping suppresses coherence of a particle, and controls its transport properties. Particularly, a particle under the ohmic damping in two-state systems shows various behaviors including coherent motion at low temperatures for weak damping, and incoherent motion in the limit of high temperatures and/or strong damping.¹⁴⁾

In this paper, we consider a particle of mass M moving in a periodic potential $V(q+a) = V(q)$ as shown in Fig. 1 (a). Here, a barrier height is denoted by V_0 , and a frequency of small oscillation around potential minima by ω_0 . The Hamiltonian of the particle is given by

$$H_S = \frac{p^2}{2M} + V(q). \quad (1.1)$$

In accordance with the Caldeira and Leggett theory,¹³⁾ we represent a dissipative environment by a set of

* Submitted to J. Phys. Soc. Jpn.

harmonic oscillators as

$$H = H_S + \sum_j \left[\frac{p_j^2}{2m_j} + \frac{1}{2} m_j \omega_j^2 \left(x_j - \frac{C_j}{m_j \omega_j^2} q \right)^2 \right]. \quad (1.2)$$

The influence of the environment is determined through the spectral density

$$J(\omega) = \frac{\pi}{2} \sum_j \frac{C_j^2}{m_j \omega_j} \delta(\omega - \omega_j). \quad (1.3)$$

The ohmic heat bath is obtained by taking $J(\omega)$ as $\eta\omega$ for $\omega \rightarrow 0$, where η is a viscosity coefficient.

In this paper, we assume $V_0 \gg \hbar\omega_0 \gg k_B T$, where k_B is the Boltzmann constant, and T is a temperature. In this parameter region, the system can be reduced to a tight binding model, which has been studied by several authors in the framework of the real-time path integral.^{21,22,23} Fisher and Zwerger have studied dynamics of a particle in a periodic potential in the weak corrugation limit ($V_0 \rightarrow 0$), and have related the results to the tight-binding model through the duality transformation,^{15,24} which is also used in the subsequent works.^{16,17} In these works, one of the important quantities is the linear mobility μ_l of the particle defined in the long-time limit $t \rightarrow \infty$ as

$$\mu_l = \lim_{F \rightarrow 0} \lim_{t \rightarrow \infty} \frac{\langle q(t) \rangle}{Ft}, \quad (1.4)$$

where F is an external force on a particle. The temperature dependence of μ_l , however, has been exactly calculated only for a special value of dimensionless damping strength, $K = 1/2$, where $K = \eta a^2 / 2\pi\hbar$.²³

In this work, we focus mainly on a weak coupling region $K \ll 1$. This region allows analytic study of the system from low to high temperatures. We calculate specific heat, and dynamical properties represented by optical conductivity $\sigma(\omega)$ and one-particle Green's functions. The linear mobility is also obtained by $\mu_l = \sigma(\omega \rightarrow 0)/e^2$. Thermodynamics of the system is formulated by the imaginary-time path integral, and transport properties are studied in the framework of the linear response theory.

Before showing the results, we comment on the justification of the Caldeira-Leggett (C-L) Hamiltonian (1.2). This phenomenological model is believed to be valid in two cases: (i) The case where the effective action of the C-L Hamiltonian agrees with the action derived from a microscopic Hamiltonian (in a proper limit of parameters) as shown in a heavy particle in a metal²⁷ and a quantum dot,¹² and (ii) the case where the classical equation of motion for the system variable q is established through experiments as studied in the Josephson devices.¹³ In addition to the above two cases, we speculate that the C-L model may be an effective model for (iii) the case of incoherent hole motion in a correlated electron system. We comment on the case (iii) in § 3.4.

The paper is organized as follows. In § 2, we derive exact formal expressions for the partition function, the optical conductivity and one-particle Green's function. We also formulate a continuous limit, an incoherent limit and a weak coupling theory for arbitrary form of $J(\omega)$. For analytical calculations, $J(\omega)$ is taken as

$$J(\omega) = \frac{2\pi\delta_s}{a^2} \left(\frac{\omega}{\tilde{\omega}} \right)^{s-1} \omega f(\omega; \omega_c), \quad (1.5)$$

where δ_s is a dimensionless coupling coefficient, and $\tilde{\omega}$ is a reference frequency. Here, $f(\omega; \omega_c)$ is a cutoff function usually taken as $f(\omega, \omega_c) = e^{-\omega/\omega_c}$, while we use a sharp cutoff, $f(\omega, \omega_c) = \Theta(\omega_c - \omega)$ in § 2.4, where $\Theta(\omega)$ is a step function. In any case, the low-frequency ($\omega \ll \omega_c$) behaviors of the dissipative particle are not influenced by the detailed form of the cut-off function. The exponent s in (1.5) mainly determines the properties of the heat bath. In § 3, we study the case $s = 1$ called ‘ohmic damping’. In the case $s > 1$ called ‘superohmic damping’, and in the case $s < 1$ called ‘subohmic damping’, calculations are so complicated that we only focus on the continuous limit (§ 2.4) and the incoherent regime (§ 2.5). Summary is given in § 4. Throughout this paper, we take $\hbar = k_B = 1$.

§2. Formulation

In this section, we give formal expressions for the partition function (§ 2.1), the optical conductivity (§ 2.2) and one-particle Green's function (§ 2.3). We also discuss a continuous limit of the tight binding model (§ 2.4). To deal with this model analytically, we focus on two limiting regions: an incoherent tunneling regime (§ 2.5) and a weak damping region (§ 2.6). In this section, the derived expressions are applicable to

Fig. 1. (a) The periodic potential studied in this paper, and (b) a representative path in the imaginary-time path integral in (2.1).

arbitrary form of $J(\omega)$.

2.1 Partition function

The exact formal expression for the partition function Z is given in the imaginary-time functional-integral representation. The integrals over the heat-bath variables are Gaussian and they can be evaluated exactly.²⁸⁾ After integrating out the degrees of freedom for the environment, the partition function is expressed as

$$Z = Z_R \oint \mathcal{D}q(\tau) \exp(-S[q(\tau)]). \quad (2.1)$$

Here, Z_R is the partition function of the heat bath, and in following calculation, Z_R is removed in order to focus only on the damping effects on the particle. The paths $q(\tau)$ satisfy the periodic boundary condition $q(\beta) = q(0)$, where $\beta = 1/T$. The effective action $S[q(\tau)]$ is given by

$$S[q(\tau)] = \int_0^\beta d\tau \left(\frac{1}{2} M \dot{q}^2 + V(q) \right) - \frac{1}{a^2} \int_0^\beta d\tau d\tau' \phi(\tau - \tau') \dot{q}(\tau) \dot{q}(\tau'). \quad (2.2)$$

Damping effects due to the heat bath are described by the last term, which takes a nonlocal form for τ . The kernel $\phi(\tau)$ is calculated as

$$\phi(\tau) = \frac{a^2}{\pi} \int_0^\infty d\omega \frac{J(\omega)}{\omega^2} (D_\omega(0) - D_\omega(\tau)), \quad (2.3)$$

$$D_\omega(\tau) = \frac{1}{\beta} \sum_{n=-\infty}^{\infty} \frac{2\omega}{\nu_n^2 + \omega^2} e^{i\nu_n \tau} \quad (2.4)$$

$$= \frac{\cosh[\omega(\beta/2 - |\tau|)]}{\sinh(\beta\omega/2)}, \quad (2.5)$$

where $\nu_n = 2\pi n/\beta$ is the Matsubara frequency.

The form of the potential $V(q)$ is shown in Fig. 1 (a). In the parameter region $T \ll \omega_0 \ll V_0$, the system is effectively mapped to a tight-binding model. In this case, the value of paths $q(\tau)$ takes $q = an$ for almost all τ , where n is an integer. A representative path is shown in Fig. 1 (b). Though the truncation scheme for the paths has already been studied in the literature,^{29, 30, 31)} we will describe it briefly for self-contained description.

In the dissipationless case, a bare hopping matrix Δ_0 is determined by the instanton action S_0 as

$$\Delta_0 = A \exp(-S_0), \quad (2.6)$$

where A is a prefactor of the order of ω_0 .³²⁾ Hence, we have a tight binding model described by the Hamil-

tonian

$$H = -\Delta_0 \sum_n \left(c_{n+1}^\dagger c_n + c_n^\dagger c_{n+1} \right), \quad (2.7)$$

where c_n (c_n^\dagger) are annihilation (creation) operators of a spinless fermion at site n . The damping effects due to the heat bath can be divided into the fast and slow modes as

$$J(\omega) = J_{\text{lf}}(\omega) + J_{\text{hf}}(\omega) \quad (2.8)$$

$$J_{\text{lf}}(\omega) = J(\omega) f(\omega; \omega_c) \quad (2.9)$$

Here, ω_c is a cutoff frequency ($\Delta_0, T \ll \omega_c \ll \omega_0$), and $f(\omega; \omega_c)$ is a cut-off function taken as $f(\omega; \omega_c) \ll 1$ for $\omega_c \ll \omega$. Then, the fast modes can be treated easily by the Born-Oppenheimer approximation. In the approximation, the bare matrix element Δ_0 is reduced to a renormalized one^{33,34}

$$\Delta = \Delta_0 \exp \left(-\frac{a^2}{2\pi} \int_0^\infty d\omega \frac{J_{\text{hf}}(\omega)}{\omega^2} \right). \quad (2.10)$$

In contrast to the fast modes, the influence of the slow modes of the heat bath must be studied carefully based on the effective action (2.2). In this paper, $J_{\text{lf}}(\omega)$ is replaced with $J(\omega)$, and Δ and ω_c are regarded as free parameters ($\Delta, T \ll \omega_c$).

Because we have already traced out the fast modes which can follow the instanton motion of the time scale $1/\omega_0$, each path $\dot{q}(\tau)$ is expressed as the sum of the delta functions as

$$\dot{q}(\tau)/a = \sum_{l=1}^{2m} \xi_l \delta(\tau - \tau_l). \quad (2.11)$$

Here, $\xi_l = \pm 1$ specifies the direction of the l -th hopping at $\tau = \tau_l$. Substituting (2.11) to (2.2), the exact formal expression of the partition function is obtained as

$$\begin{aligned} Z &= \sum_{m=0}^{\infty} \Delta^{2m} \sum_{\{\xi_l\}'} \int_0^\beta d\tau_{2m} \int_0^{\tau_{2m}} d\tau_{2m-1} \cdots \int_0^{\tau_2} d\tau_1 \exp \left[\sum_{k<l}^{2m} \xi_k \xi_l \phi(\tau_l - \tau_k) \right] \\ &= \sum_{m=0}^{\infty} \frac{\Delta^{2m}}{2m!} \sum_{\{\xi_l\}'} \prod_{n=1}^{2m} \int_0^\beta d\tau_n \exp \left[\sum_{k<l}^{2m} \xi_k \xi_l \phi(\tau_l - \tau_k) \right]. \end{aligned} \quad (2.12)$$

Here, the prime in $\{\xi_l\}'$ denotes summation in accordance with the constraint

$$\sum_{l=1}^{2m} \xi_l = 0. \quad (2.13)$$

The expression (2.12) may be interpreted as the statistical model of the classical particles interacting to the τ -direction with the potential $-\phi(\tau)$.²⁴ In this point of view, Δ and ξ_l are regarded as a chemical potential and a charge of a particle. The inverse temperature $\beta = 1/T$ in the original model corresponds to the system length in the τ direction, and the constraint (2.13) is interpreted as the condition for the charge neutrality. The mapping to the classical statistical mechanics is useful for constituting the weak coupling theory. Actually, the ‘screening effect’ by charged particles is important to describe transport properties of the original model at low temperatures. (See § 2.6.)

2.2 Optical conductivity

We formulate the optical conductivity $\sigma(\omega)$ in one dimension using the Kubo formula³⁵

$$\sigma(\omega) = -e^2 a^2 \frac{\langle -\mathcal{K} \rangle - \Lambda(\omega)}{i(\omega + i\delta)}, \quad (2.14)$$

where δ is an adiabatic constant, and \mathcal{K} is a kinetic energy

$$\mathcal{K} = -\Delta \sum_n \left(c_{n+1}^\dagger c_n + c_n^\dagger c_{n+1} \right), \quad (2.15)$$

and a current-current correlation function $\Lambda(\omega)$ is defined by

$$\Lambda(\omega) = \tilde{\Lambda}(i\omega_m \rightarrow \omega + i\delta). \quad (2.16)$$

$$\tilde{\Lambda}(i\omega_m) = \int_0^\beta d\tau e^{i\omega_m \tau} \langle j(\tau)j(0) \rangle, \quad (2.17)$$

Here, the current operator $j(\tau) = e^{\tau H} j e^{-\tau H}$ is defined by

$$j = i\Delta \sum_n \left(c_{n+1}^\dagger c_n - c_n^\dagger c_{n+1} \right). \quad (2.18)$$

The real part of $\sigma(\omega)$ contains a coherent part expressed by a delta function as^{36,37)}

$$\text{Re } \sigma(\omega) = D\delta(\omega) + \sigma_{\text{res}}(\omega). \quad (2.19)$$

Here, D is called a Drude weight, and $\sigma_{\text{res}}(\omega)$ is a residual incoherent part. From (2.14), we obtain

$$\frac{D}{\pi e^2 a^2} = \langle -\mathcal{K} \rangle - \text{Re } \Lambda(\omega \rightarrow 0), \quad (2.20)$$

$$\sigma_{\text{res}}(\omega) = e^2 a^2 \frac{\text{Im } \Lambda(\omega)}{\omega}. \quad (2.21)$$

To evaluate $\Lambda(\omega)$, we consider the imaginary-time correlation function $\tilde{\Lambda}(\tau) = \langle j(\tau)j(0) \rangle$. The correlation function is formulated by the imaginary-time path integral as

$$\tilde{\Lambda}(\tau) = \frac{\Delta^2}{Z} \oint \mathcal{D}' q(\tau') \exp[-S[q(\tau')]]. \quad (2.22)$$

Here, the path integral is performed over all the possible paths $q(\tau)$ with two jumps at $\tau' = 0, \tau$ as

$$\dot{q}(\tau')/a = \sum_{l=1}^{2m} \xi_l \delta(\tau' - \tau_l) + \sigma \delta(\tau') + \sigma' \delta(\tau' - \tau), \quad (2.23)$$

where $2m+2$ is the number of transitions, and $\xi_l, \sigma, \sigma' = \pm 1$ denote the directions of hopping at $\tau' = \tau_l, 0, \tau$. Then, the path integral is expressed as

$$\oint \mathcal{D}' q(\tau')(\dots) = \sum_{m=0}^{\infty} \sum_{\{\xi_l, \sigma, \sigma'\}'} (-\sigma\sigma') \frac{1}{2m!} \prod_{l=1}^{2m} \int_0^\beta d\tau_l(\dots). \quad (2.24)$$

Here, the prime in $\{\xi_l, \sigma, \sigma'\}'$ denotes the summation in accordance with the constraint

$$\sum_{l=1}^{2m} \xi_l + \sigma + \sigma' = 0, \quad (2.25)$$

which comes from the periodic boundary condition for $q(\tau')$. Here, we divide $\Lambda(\omega)$ into two parts as

$$\tilde{\Lambda}(\tau) = \tilde{\Lambda}_1(\tau) - \tilde{\Lambda}_2(\tau), \quad (2.26)$$

where $\tilde{\Lambda}_1(\tau)$ and $\tilde{\Lambda}_2(\tau)$ denote the contribution of paths which satisfy $\sigma = -\sigma'$ and $\sigma = \sigma'$, respectively. From (2.22)-(2.24), we obtain

$$\begin{aligned} \tilde{\Lambda}_1(\tau) &= \frac{2\Delta^2}{Z} \sum_{m=0}^{\infty} \frac{\Delta^{2m}}{2m!} \sum_{\{\xi_l\}'} \int_0^\beta \prod_{l=1}^{2m} d\tau_l \\ &\quad \times \exp \left(\sum_{k<l}^{2m} \xi_k \xi_l \phi(\tau_l - \tau_k) + \sum_{l=1}^{2m} \xi_l \phi(\tau_l) - \sum_{l=1}^{2m} \xi_l \phi(\tau_l - \tau) - \phi(\tau) \right). \quad (2.27) \\ \tilde{\Lambda}_2(\tau) &= \frac{2\Delta^2}{Z} \sum_{m=0}^{\infty} \frac{\Delta^{2m}}{2m!} \sum_{\{\xi_l\}''} \int_0^\beta \prod_{l=1}^{2m} d\tau_l \end{aligned}$$

$$\times \exp \left(\sum_{k < l}^{2m} \xi_k \xi_l \phi(\tau_l - \tau_k) + \sum_{l=1}^{2m} \xi_l \phi(\tau_l) + \sum_{l=1}^{2m} \xi_l \phi(\tau_l - \tau) + \phi(\tau) \right). \quad (2.28)$$

Here, the prime in $\{\xi_l\}'$ and the double prime in $\{\xi_l\}''$ denote the summations in accordance with (2.13) and the condition

$$\sum_{l=1}^{2m} \xi_l + 2 = 0, \quad (2.29)$$

respectively. From (2.27) and (2.28), $\tilde{\Lambda}_1(\tau)$ and $\tilde{\Lambda}_2(\tau)$ can be interpreted as the partition functions with fixed charges at $\tau' = 0, \tau$ in terms of the classical partition function (2.12).

We can calculate $\sigma_{\text{res}}(\omega) = e^2 a^2 \text{Im} \Lambda(\omega) / \omega$ without the Wick rotation (2.16). We introduce a real-time correlation function as

$$\begin{aligned} \Lambda(t) &= i\Theta(t) \langle j(t)j(0) - j(0)j(t) \rangle \\ &= -2\text{Im} \tilde{\Lambda}(\tau \rightarrow it), \end{aligned} \quad (2.30)$$

where $j(t) = e^{iHt} j e^{-iHt}$. Then, the correlation function $\Lambda(\omega)$ is given by

$$\Lambda(\omega) = \int_0^\infty dt \Lambda(t) e^{i\omega t}. \quad (2.31)$$

The above expressions, (2.30) and (2.31), are used to the calculation in the incoherent region and the weak-coupling region. We should note that the causality, $\Lambda(t) = 0$ for $t < 0$, gives the frequency sum-rule³⁸⁾

$$\int_{-\infty}^\infty d\omega \text{Re} \sigma(\omega) = \pi e^2 a^2 \langle -\mathcal{K} \rangle. \quad (2.32)$$

The sum rule is always satisfied in the approximations adopted in this paper, since the causality is always satisfied.

2.3 One-particle Green's function

In this subsection, we consider the Green's function of the dissipative particle. First, we define the imaginary-time Green's function as

$$\tilde{G}_{ij}(\tau) = -\langle T_\tau c_i(\tau) c_j^\dagger(0) \rangle_{\text{R}}, \quad (2.33)$$

where T_τ is the time-ordered product. The thermal average $\langle \cdots \rangle_{\text{R}}$ is defined by

$$\langle \cdots \rangle_{\text{R}} = \frac{\text{Tr}_{\text{R}} [e^{-\beta H_{\text{R}}} \cdots]}{\text{Tr}_{\text{R}} [e^{-\beta H_{\text{R}}}]}, \quad (2.34)$$

where H_{R} is the Hamiltonian of the heat bath. The trace Tr_{R} is taken in the Hilbert space spanned by all state of the heat bath and the empty state for the dissipative particle. Then, the Green's function is expressed as

$$\tilde{G}_{ij}(\tau) = -\frac{1}{Z_{\text{R}}} \text{Tr}_{\text{R}} \left[e^{-(\beta-\tau)H_{\text{R}}} c_i e^{-\tau H} c_j^\dagger \right] \quad (2.35)$$

$$= -\int_0^\tau \mathcal{D}q(\tau) \exp(-S_{\text{eff}}[q(\tau)]), \quad (2.36)$$

where H is the total Hamiltonian including damping effects. In the second equation, the variables of the heat bath are traced out. The path integral is performed in accordance with the boundary condition

$$q(0)/a = j, \quad q(\tau)/a = i, \quad (2.37)$$

The Green's function depends only on $L = i - j$. The paths are expressed discretely as

$$\dot{q}(\tau')/a = \sum_{l=1}^{2m+L} \xi_l \delta(\tau' - \tau_l) - L\delta(\tau'), \quad (2.38)$$

where $\xi_l (= \pm 1)$ satisfy

$$\sum_{l=1}^{2m+L} \xi_l = L. \quad (2.39)$$

By substituting (2.38) to (2.36), we obtain

$$\tilde{G}_{i,i+L}(\tau) = - \sum_{m=0}^{\infty} \frac{\Delta^{2m+L}}{2m!} g_{L,m}, \quad (2.40)$$

$$g_{L,m} = \sum_{\{\xi_l\}'''} \prod_{n=1}^{2m+L} \int_0^\tau d\tau_n \exp \left[\sum_{k<l}^{2m+L} \xi_k \xi_l \phi(\tau_l - \tau_k) + L \sum_{l=1}^{2m+L} \xi_l \phi(\tau_l) \right], \quad (2.41)$$

where the triple prime in $\{\xi_l\}'''$ denotes the summation in accordance with (2.39).

Here, $g_{L,m}$ can be interpreted as the partition function of classical plasma consisting of the ‘fixed’ particle with charge L at $\tau' = 0$ and additional $2m + L$ particles. Therefore, the weak coupling theory based on the Debye-Hückel approximation can also be applied to $\tilde{G}_{i,i+L}(\tau)$. (See § 2.6.)

2.4 Continuum limit

In the dissipationless case, the energy dispersion is given by

$$\varepsilon_k = -2\Delta \cos ka, \quad (2.42)$$

where k is a momentum. The lattice model is reduced to the continuum model in the limit $a \rightarrow 0$ ($\Delta \rightarrow \infty$) by keeping $\bar{M} = 1/2\Delta a^2$ constant. In this limit, the energy dispersion is approximated as

$$\varepsilon_k \simeq -2\Delta + \frac{k^2}{2\bar{M}}. \quad (2.43)$$

Note that the mass \bar{M} is not necessarily the same as the bare mass M in the original Hamiltonian. In the continuum limit $\Delta \rightarrow \infty$, thermal fluctuations may be neglected ($T/\Delta \rightarrow 0$). Hence, the continuum limit corresponds to the zero-temperature limit.

Next, we consider the dissipative case. In the continuum limit, the classical equation of motion for the average position $\langle q(t) \rangle$ is obtained by virtue of Ehrenfest’s theorem as

$$\langle \ddot{q}(t) \rangle + \int_{-\infty}^t dt' \gamma(t-t') \langle \dot{q}(t') \rangle = \frac{e}{M} E(t), \quad (2.44)$$

where $E(t)$ is an external electric field. The damping kernel $\gamma(t)$ is determined by the spectral density $J(\omega)$ as^{1,20)}

$$\gamma(t) = \int_{-\infty}^{\infty} \frac{d\omega}{2\pi} e^{-i\omega t} \tilde{\gamma}(z \rightarrow -i\omega + \delta), \quad (2.45)$$

$$\tilde{\gamma}(z) = \frac{2z}{\pi \bar{M}} \int_0^{\infty} d\omega' \frac{J(\omega')}{\omega'(\omega'^2 + z^2)}. \quad (2.46)$$

From the classical equation (2.44), the Fourier transformation of the current $j(t) = e\langle \dot{q}(t) \rangle$ gives $\tilde{j}(\omega) = \sigma(\omega) \tilde{E}(\omega)$, and the optical conductivity $\sigma(\omega)$ is given by

$$\sigma(\omega) = \frac{e^2}{\bar{M}(z + \tilde{\gamma}(z))} \Big|_{z \rightarrow -i\omega + \delta}. \quad (2.47)$$

Because of the causality, the sum rule (2.32) is also satisfied in the continuum limit.

The above result is valid for any form of the spectral density $J(\omega)$. Here, we take $J(\omega)$ as

$$J(\omega) = \bar{M} \gamma_s \left(\frac{\omega}{\tilde{\omega}} \right)^{s-1} \omega \Theta(\omega_c - \omega), \quad (2.48)$$

where $\gamma_s = 2\pi\delta_s/a^2\bar{M} = 4\pi\delta_s\Delta$ is a damping frequency, and the cut-off function $f(\omega; \omega_c)$ in (1.5) is taken as the step function $\Theta(\omega_c - \omega)$ for convenience. The characteristic damping frequency $\tilde{\gamma}$ is determined by $\tilde{\gamma} = (\gamma_s \tilde{\omega}^{1-s})^{1/(2-s)}$. To keep $\tilde{\gamma}$ constant in the continuum limit $\Delta \rightarrow \infty$, the dimensionless coupling

coefficient $\delta_s = \gamma_s/4\pi\Delta$ must be suppressed to zero. Hence, the continuum limit corresponds to the weak coupling limit $\delta_s \rightarrow 0$.

From (2.48), the damping kernel $\hat{\gamma}(\omega)$ in (2.46) is calculated analytically. The leading term is given by²⁰⁾

$$\hat{\gamma}(z) = \begin{cases} \frac{\gamma_s}{\sin(\pi s/2)} \left(\frac{z}{\tilde{\omega}}\right)^{s-1} [1 + \mathcal{O}(z/\omega_c, (z/\omega_c)^{2-s})], & (0 < s < 2), \\ \frac{\gamma_s z}{\pi \tilde{\omega}} \ln\left(1 + \frac{\omega_c^2}{z^2}\right), & (s = 2), \\ \frac{2\gamma_s}{\pi(s-2)} \left(\frac{\omega_c}{\tilde{\omega}}\right)^{s-2} \frac{z}{\tilde{\omega}} (1 + \mathcal{O}(z^2/\omega_c^2, (z/\omega_c)^{s-2})), & (s > 2). \end{cases} \quad (2.49)$$

From (2.47) and (2.49), it is proved that the delta function disappears at $\omega = 0$ in $\text{Re } \sigma(\omega)$ for $0 < s < 2$. This result strongly indicates that the Drude weight D in (2.19) vanishes for $0 < s < 2$ at all temperatures and damping coefficients. This is because the continuum limit describes the low-temperature and weak-coupling limit, $T, \delta_s \rightarrow 0$, while this limit should give the most coherent result in the parameter space. On the other hand, the Drude weight appears for $s > 2$, and the damping effects appears only in the mass renormalization

$$\bar{M} \rightarrow \bar{M} \left(1 + \frac{2}{\pi(s-2)} \frac{\gamma_s}{\tilde{\omega}} \left(\frac{\omega_c}{\tilde{\omega}}\right)^{s-2}\right). \quad (2.50)$$

In this case, the residual conductivity for $\omega > 0$ vanishes. The above result is related to the Brownian motion caused by a heat bath, where the long time behavior of $\langle (q(t) - q(0))^2 \rangle$ at finite temperatures is proportional to t^2 for $s > 2$, and t^s for $s < 2$. The transition at $s = 2$ can be understood by a simple discussion on the mass renormalization expressed in general as^{19,20)}

$$\bar{M} \rightarrow \bar{M} + \frac{2}{\pi} \int_0^\infty d\omega \frac{J(\omega)}{\omega^3}. \quad (2.51)$$

When this integral is convergent, the particle motion becomes coherent in the continuum limit.

Let us see the s dependence in more detail. The residual part $\sigma_{\text{res}}(\omega)$ appears only for the case $s \leq 2$. From (2.47) and (2.49), we obtain

$$\sigma_{\text{res}}(\omega) = \frac{e^2}{M\tilde{\gamma}} \frac{\left(\frac{\omega}{\tilde{\gamma}}\right)^{s-1}}{\left(\frac{\omega}{\tilde{\gamma}} - \cot \frac{\pi s}{2} \left(\frac{\omega}{\tilde{\gamma}}\right)^{s-1}\right)^2 + \left(\frac{\omega}{\tilde{\gamma}}\right)^{2(s-1)}}, \quad (2.52)$$

where $\tilde{\gamma} = (\gamma_s \tilde{\omega}^{1-s})^{1/(2-s)}$. In this case, $\sigma_{\text{res}}(\omega)$ behaves qualitatively as

$$\sigma_{\text{res}}(\omega) \sim \begin{cases} \omega^{1-s} & (\omega < \tilde{\gamma}), \\ \omega^{s-3} & (\omega > \tilde{\gamma}). \end{cases} \quad (2.53)$$

The ω -dependence of $\sigma_{\text{res}}(\omega)$ for $s = 0.5, 1, 1.5$ is shown in Fig. 2. For subohmic damping $0 < s < 1$, the conductivity is reduced to zero as ω decreases. On the other hand, in the superohmic case $1 < s < 2$, the conductivity diverges for $\omega \rightarrow 0$. For the ohmic damping $s = 1$, the optical conductivity $\sigma_{\text{res}}(\omega)$ takes a simple Drude form.

As s increases toward 2, the curve of $\sigma_{\text{res}}(\omega)$ approaches the $1/\omega$ form. The case of $s = 2$ is marginal, and we obtain

$$\sigma_{\text{res}}(\omega) = \frac{e^2 \gamma_2}{M\omega\tilde{\omega}} \frac{1}{\left(1 + \frac{\gamma_2}{\pi\tilde{\omega}} \log\left|\frac{\omega_c^2}{\omega^2} - 1\right|\right)^2 + \left(\frac{\gamma_2}{\tilde{\omega}}\right)^2}, \quad (\omega < \omega_c). \quad (2.54)$$

The optical conductivity $\sigma_{\text{res}}(\omega)$ behaves nearly as $1/\omega$ for $\omega \ll \omega_c$. For $s > 2$, the incoherent part vanishes, and the delta function appears in $\text{Re } \sigma(\omega)$.

2.5 Incoherent tunneling regime

In the limit of high temperatures and/or strong damping, the particle moves incoherently to the neighbor sites. In this regime, the occupation probabilities obey a simple master equation,^{15,21)} and the hopping rate is formulated by the Fermi's golden rule, where the incoherent motion of the particle is described by the

Fig. 2. The optical conductivity $\sigma(\omega)$ in the continuum limit for $s = 0.5, 1, 1.5$. Particularly, for the ohmic damping $s = 1$, $\sigma(\omega)$ takes a simple Drude form.

term of order of Δ^2 in the correlation function. From (2.26)-(2.28), the relevant term is given by

$$\tilde{\Lambda}(\tau) = 2\Delta^2 \exp[-\phi(\tau)]. \quad (2.55)$$

From (2.30), the real-time correlation function $\Lambda(t)$ is derived as

$$\Lambda(t) = 4\Delta^2 \sin R(t) \exp(-S(t)), \quad (2.56)$$

where $S(t)$ and $R(t)$ are real functions defined by $\phi(\tau = it) = S(t) + iR(t)$. The explicit form of $S(t)$ and $R(t)$ is given from (2.3) and (2.5) as

$$S(t) = \frac{a^2}{\pi} \int_0^\infty d\omega \frac{J(\omega)}{\omega^2} (1 - \cos \omega t) \coth \frac{\beta\omega}{2}, \quad (2.57)$$

$$R(t) = \frac{a^2}{\pi} \int_0^\infty d\omega \frac{J(\omega)}{\omega^2} \sin \omega t. \quad (2.58)$$

The Fourier transformation of (2.56) gives

$$\text{Im } \Lambda(\omega) = 4\Delta^2 \int_0^\infty dt \sin \omega t \sin R(t) \exp(-S(t)). \quad (2.59)$$

Thus, the optical conductivity is calculated from $\sigma_{\text{res}}(\omega) = e^2 a^2 \text{Im } \Lambda(\omega) / \omega$. The formulation of the incoherent region is valid only when the integral (2.59) is convergent.

The above formulation is quite similar to the calculation of the nonlinear mobility in biased periodic-potential systems.²⁵⁾ Actually, the tunneling rate $\Gamma(\varepsilon)$ and the nonlinear mobility $\mu(\varepsilon)$ with a bias ε are calculated in these systems as

$$\Gamma(\varepsilon) = 4\Delta^2 \int_0^\infty dt \cos \varepsilon t \sin R(t) \exp(-S(t)), \quad (2.60)$$

$$\mu(\varepsilon) = \frac{4a^2\Delta^2}{\varepsilon} \int_0^\infty dt \sin \varepsilon t \sin R(t) \exp(-S(t)). \quad (2.61)$$

Compared (2.61) with (2.59), the optical conductivity is obtained as $\sigma_{\text{res}}(\omega) = e^2 \mu(\varepsilon \rightarrow \omega)$. Further, it is proved that μ is related to Γ through the relation²⁵⁾

$$\mu = a^2 \tanh(\beta\varepsilon/2) \Gamma / \varepsilon. \quad (2.62)$$

Thus, we can obtain the optical conductivity from the tunneling rate $\Gamma(\varepsilon)$ as

$$\sigma_{\text{res}}(\omega) = e^2 a^2 \frac{\tanh(\beta\omega/2)}{\omega} \Gamma(\varepsilon \rightarrow \omega). \quad (2.63)$$

In order to calculate $\Gamma(\varepsilon)$ in the incoherent regime, we can utilize the results on two-state systems obtained

in ref. 14, where the tunneling rate is formulated by the same form as (2.60), and is calculated for a few regions in the parameter space. For the ohmic damping, it is proved that the expansion in terms of Δ gives the systematic high-temperature expansion. We consider the lowest contribution of order of Δ^2 in § 3. In the subohmic case ($0 < s < 1$) and the superohmic case ($1 < s < 2$), the calculation is so complicated that analytical treatment is possible only in the limiting cases. The results are given in Appendix A, and we do not discuss the other cases in this paper. We note that the result (2.59) is also related to the transition rate of the photo-induced tunneling in the two-level systems.²⁹⁾

In the incoherent tunneling regime, the partition function (2.12) is also approximated as

$$Z = 1 + 2\beta\Delta^2 \int_0^\beta d\tau \exp[-\phi(\tau)]. \quad (2.64)$$

This form corresponds to the partition function of dissipative two-state systems except a difference of a factor 2 which comes from two possible transitions to neighbor sites.²⁶⁾

2.6 Weak coupling theory

For weak damping ($\delta_s \ll 1$), analytical calculation is possible for all temperatures. We, however, should be careful to constitute the weak coupling theory, because we must deal with screening effects of interacting charged particles described in (2.12). In order to treat the screening effects, we adopt the ‘ring approximation’, which is proved to be equivalent to the Debye-Hückel theory. Since this approximation is believed to be valid in the weak coupling region, we expect that reliable results is obtained in the weak damping region by this approximation. In this subsection, we derive the partition function, the optical conductivity and one-particle Green’s function based on the ring approximation. Since details of the calculation are straightforward, but rather tedious, we show only the results here. Details of the calculation are given in Appendix B and C.

2.6.1 Partition function

First, we define a Fourier transformation of the potential $\phi(\tau)$ as

$$\phi(i\omega_m) = \int_0^\beta d\tau e^{i\omega_m\tau} \phi(\tau), \quad (2.65)$$

where $\omega_m = 2\pi m/\beta$ is the Matsubara frequency. By comparing (2.3)-(2.4) with (2.46), $\phi(i\omega_m)$ can be related to the damping kernel $\hat{\gamma}(z)$ for $\omega_m \neq 0$ as

$$\phi(i\omega_m) = -\frac{\bar{M}a^2}{\omega_m} \hat{\gamma}(z = \omega_m). \quad (2.66)$$

To avoid unphysical divergence, we shift the potential $\phi(\tau)$ by the zero frequency component $\phi_0 = \phi(i\omega_m = 0)$ as

$$\phi(i\omega_m) \rightarrow \phi(i\omega_m) + \phi_0. \quad (2.67)$$

By the potential shift, the transition amplitude Δ is renormalized as

$$\bar{\Delta} = \Delta \exp\left(-\frac{1}{2}\phi_0\right), \quad (2.68)$$

where the factor $\exp(-\phi_0/2)$ corresponds to the Frank-Condon factor. Details of calculation for ϕ_0 is given in Appendix B.

From the approximate calculation given in Appendix C, the analytical form of the partition function is obtained as

$$Z = \int_0^{2\pi} \frac{d\theta}{2\pi} \exp[U(n)] \quad (2.69)$$

$$U(n) = n + \int_0^n dn Q(n) - nQ(n), \quad (2.70)$$

$$Q(n) = \frac{1}{\beta^2} \sum_{\omega_m > 0} \frac{n\phi(i\omega_m)^2}{1 - n\phi(i\omega_m)/\beta}, \quad (2.71)$$

where $n = n(\theta)$ is determined by the equation

$$2\beta\bar{\Delta} \cos \theta = ne^{-Q(n)}. \quad (2.72)$$

From eqs. (2.69)-(2.72), the partition function Z is calculated analytically at least for the ohmic damping. (See § 3.2.)

2.6.2 Optical conductivity

The ring approximation is also applicable to the conductivity $\sigma(\omega)$. When we define a screened potential $\varphi(\tau; \theta)$ as

$$\varphi(\tau; \theta) = \frac{1}{\beta} \sum_{i\omega_m} \frac{\phi(i\omega_m)}{1 - n(\theta)\phi(i\omega_m)/\beta} e^{-i\omega_m\tau}, \quad (2.73)$$

the correlation functions are expressed as

$$\tilde{\Lambda}(\tau) = \tilde{\Lambda}_1(\tau) - \tilde{\Lambda}_2(\tau) \quad (2.74)$$

$$\tilde{\Lambda}_1(\tau) = \frac{1}{2Z} \int_0^{2\pi} \frac{d\theta}{2\pi} \frac{n^2}{\beta^2 \cos^2 \theta} \exp[U(\theta) - \varphi(\tau; \theta)], \quad (2.75)$$

$$\tilde{\Lambda}_2(\tau) = \frac{1}{2Z} \int_0^{2\pi} \frac{d\theta}{2\pi} \frac{n^2}{\beta^2 \cos^2 \theta} \exp[U(\theta) + 2i\theta + \varphi(\tau; \theta)]. \quad (2.76)$$

After the replacement $\tau \rightarrow it$, the screened potential is expressed by

$$\varphi(it; \theta) = S(t; \theta) + iR(t; \theta), \quad (2.77)$$

where $S(t; \theta)$ is a real part, and $R(t; \theta)$ is an imaginary part. Using this notation, the real-time correlation function in (2.30) is written by

$$\Lambda(t) = \frac{1}{Z} \int_0^{2\pi} \frac{d\theta}{2\pi} \frac{n^2}{\beta^2 \cos^2 \theta} e^{U(\theta)} \left[e^{-S(t; \theta)} + e^{S(t; \theta)} \cos 2\theta \right] \sin R(t; \theta). \quad (2.78)$$

Thus, the optical conductivity is calculated from (2.21) and (2.31).

In the high-temperature limit ($\beta \rightarrow \infty$), the screened potential (2.73) agrees with the unscreened potential $\phi(\tau)$, because the second term of the denominator in (2.73) is suppressed. Therefore, the expressions of the weak coupling region is consistently connected to the formulation in the incoherent regime, (2.55).

In the limit $T, \delta_s \rightarrow 0$, the weak coupling must correspond to the continuum limit. To see the relation, it is convenient to study the imaginary-time correlation function $\tilde{\Lambda}(\tau)$. In the continuum limit, the dimensionless coupling coefficient δ_s is reduced to zero. Therefore, the screened potential $\varphi(\tau)$ becomes small, and the approximation

$$\exp(\pm\varphi(\tau)) \simeq 1 \pm \varphi(\tau) \quad (2.79)$$

is justified. From (2.74)-(2.76), the imaginary-time correlation function is calculated approximately as

$$\tilde{\Lambda}(i\omega_m) = -\frac{1}{2Z} \int_0^{2\pi} \frac{d\theta}{2\pi} \frac{n^2}{\beta^2 \cos^2 \theta} e^{U(\theta)} (1 + e^{2i\theta}) \frac{\phi(i\omega_m)}{1 - n(\theta)\phi(i\omega_m)/\beta}. \quad (2.80)$$

The continuum limit ($\Delta \rightarrow \infty$) corresponds also to the zero temperature limit ($T/\Delta \rightarrow 0$). In the zero temperature limit, the contribution at $\theta = 0$ is dominant in the integral (2.80). Further, from (2.72), n is evaluated by $n = 2\beta\Delta$. Thus, we obtain

$$\tilde{\Lambda}(i\omega_m) = \frac{1}{\bar{M}a^2} \frac{\hat{\gamma}(\omega_m)}{\omega_m + \hat{\gamma}(\omega_m)}, \quad (2.81)$$

where $\bar{M} = 1/2\Delta a^2$ and the relation (2.66) is used. From (2.81), the optical conductivity in the continuum limit is obtained as

$$\sigma_{\text{res}}(\omega) = e^2 a^2 \text{Im} \frac{\tilde{\Lambda}(i\omega_m \rightarrow \omega + i\delta)}{\omega} \quad (2.82)$$

$$= \frac{e^2}{\bar{M}} \text{Re} \left. \frac{1}{z + \hat{\gamma}(z)} \right|_{z \rightarrow -i\omega + \delta}. \quad (2.83)$$

This expression corresponds to the optical conductivity in the continuum limit, (2.47).

2.6.3 One-particle Green's function

By using the ring approximation, the Green's function given by (2.40)-(2.41) is approximately calculated in a compact form

$$\tilde{G}_{i,i+L}(\tau) = -e^{-L^2\phi_0/2} \int_0^{2\pi} \frac{d\theta}{2\pi} e^{-iL\theta + U(\theta) + L^2Q(\theta)}, \quad (2.84)$$

where $U(\theta)$ and $Q(\theta)$ is defined by (2.70) and (2.71). (For details of the calculation, see Appendix. C) Note that the Green's function includes the potential shift ϕ_0 . As a result, in the ohmic damping case, the Green's function is suppressed to zero for $L \neq 0$ in the limit $\omega_c \rightarrow \infty$. (See § 3.)

§3. Ohmic Damping

3.1 General review of ohmic damping

In this section, we consider the ohmic damping case, in which the spectral density is described as

$$J(\omega) = \frac{2\pi K}{a^2} \omega e^{-\omega/\omega_c}. \quad (3.1)$$

Here, K is a dimensionless coupling constant. The Fourier component of the potential in (2.3) is calculated as

$$\phi(i\omega_m) = \begin{cases} -\frac{2\pi K}{|\omega_m|}, & (0 < |\omega_m| \ll \omega_c), \\ 2K \log \frac{\beta\omega_c}{2\pi}, & (\omega_m = 0). \end{cases} \quad (3.2)$$

The calculation of $\phi_0 = \phi(i\omega_m = 0)$ is given in Appendix B. From (3.2), the renormalized hopping amplitude $\bar{\Delta}$ in (2.68) is given by

$$\bar{\Delta} = \Delta \left(\frac{\beta\omega_c}{2\pi} \right)^{-K}. \quad (3.3)$$

In the following subsections, we calculate the specific heat, the optical conductivity and one-particle Green's function for the ohmic dissipation. Before showing the results, we briefly review previous works on the properties of the ohmic dissipation.

For two-state systems, nonequilibrium behaviors of the dissipative particle have been studied by Leggett *et al.*¹⁴⁾ They have calculated the real-time evolution of the expectation of the particle position with the Non-Interacting Blip Approximation (NIBA). The properties of the system are determined by the damping strength K and the temperature T , where the phase diagram obtained by NIBA is given in Fig. 3. There exist two regions in the phase diagram. In the 'incoherent' region, the particle moves incoherently, and the expectation value of the position, $\langle q(t) \rangle$ decays exponentially to the thermal equilibrium state. On the other hand, in the 'coherent' region, $\langle q(t) \rangle$ shows damped oscillation. We should note that several different definitions of the terms, 'coherent' and 'incoherent', are possible.⁴¹⁾ For example, in the numerical study of equilibrium properties of dissipative two-state systems,^{39,40)} the term 'incoherence' is defined by disappearance of an inelastic peak of the response function, which is observed at $K > 0.33$. Also in this paper, a different definition of the term, 'incoherence' is adopted in § 3.4.

As compared with the two-state systems, it is more difficult to solve the lattice model studied in this paper. For example, the simple approximation such as NIBA is not applicable to the lattice model. The dissipative particle in the tight-binding model has been studied within the real-time path integral formulation in detail.^{21,22,23)} Particularly, early discussions are based on the the duality transformation, which relates the tight-binding model to the periodic-potential system in a weak corrugation limit.^{15,16,17,24)} In these works, only the mobility of the dissipative particle has been of interest, and the whole dynamical properties of equilibrium states such as the optical conductivity have not been considered. Further, the mobility at intermediate temperatures has not been obtained exactly except for the special value of the damping strength ($K = 1/2$).

In this paper, we consider mainly two limiting regions in the phase diagram. The first one is the weak damping region $K \ll 1$, which allows analytical treatment at all temperatures. The formulation of the weak damping theory can connect the low-temperature 'coherent' region to the high-temperature 'incoherent' region in a natural way. The result obtained in this narrow region will also be useful to understand properties

Fig. 3. The phase diagram of dissipative two-state systems for the ohmic damping. This phase diagram has been obtained by the Non-Interacting Blip Approximation adopted in ref. 14. In the ‘coherent’ region, the expectation value of the position, $\langle q(t) \rangle$ shows oscillations, while in the ‘incoherent’ region, $\langle q(t) \rangle$ shows the exponential decay. The regions which allow analytical treatments is also shown: the weak coupling regime and the solvable line ($K = 1/2$). The localization-delocalization transition at $T = 0$ is also drawn.

	Low-temperature and weak-damping region	High-temperature or/and strong damping
Specific heat C	$\propto T/K$	$\propto \begin{cases} T^{-2+2K} & (K < 3/2) \\ T & (K > 3/2) \end{cases}$
Optical conductivity $\sigma(\omega)$	$\propto \begin{cases} \omega^{-2+2K} & (\omega \gg \gamma_0) \\ \text{const.} & (\omega \ll \gamma_0) \end{cases}$	$\propto \begin{cases} \omega^{-2+2K} & (\omega \gg KT) \\ T^{-2+2K} & (\omega \ll KT) \end{cases}$
DC conductivity σ_{DC}	$\propto 1 - \text{const.}T^2$	$\propto T^{-2+2K}$
Green’s function $G(k, \omega)$	k -independent	k -independent

Table I. Summary of the results. Here, K is the dimensionless damping coefficient, and γ_0 is the damping frequency defined by (3.31).

in the other region. The second region is the high-temperature and/or strong damping region. In this limit, the dissipative particle moves incoherently with the hopping rate determined mainly by the Fermi’s golden rule. Especially, in the region $K > 1$, the high temperature expansion is convergent, and the Fermi’s golden rule gives the leading term at all temperatures. On the other hand, for $K < 1$, the high temperature expansion fails below the Kondo temperature T_K . The summary of the results on these two region is given in Table I.

With regard to the optical conductivity, the result on the continuum limit is also useful to understand the general behavior. The continuum limit corresponds to the low-temperature and weak-coupling limit ($K, T \rightarrow 0$), and the particle is expected to move coherently. From (2.52), the optical conductivity in the continuum limit is calculated as a simple Drude form

$$\sigma_{\text{res}}(\omega) = \frac{e^2 \gamma}{M(\omega^2 + \gamma^2)}. \quad (3.4)$$

When the finite damping is introduced, the optical conductivity deviates from the Drude form (3.4). This behavior is studied in detail in § 3.3.

In addition to the above regions, it is expected that the calculation at $K = 1/2$ is tractable analytically by following ref. 23, though we do not deal with the case in this paper. In the other regions (particularly

Fig. 4. The specific heat for weak damping ($K = 0.03, 0.06, 0.1, 0.15$). The specific heat is suppressed to zero as the temperature decreases. This behavior is quite different from the dissipationless case ($K = 0$), where the specific heat approaches a nonzero constant at low temperatures.

for $0 < K < 1$), the analytical method cannot be used. Hence, the dynamical properties of these region will have to be studied by numerical calculation, which has not been performed before to the lattice model within our knowledge.

Finally, we comment on the renormalization of Δ due to the damping. For the ohmic damping, the relevant frequency of the system is given by

$$\Delta_{\text{eff}} = \Delta \left(\frac{\Delta}{\omega_c} \right)^{K/(1-K)}, \quad (3.5)$$

for $0 < K < 1$. The frequency gives the scale of the Kondo temperature T_K . By rewriting Δ_{eff} as Δ , the final results can be expressed without the cutoff frequency ω_c .¹⁴⁾ In this paper, all the results are expressed by Δ_{eff} finally.

3.2 Specific heat

In this subsection, we consider the specific heat of the system coupled to the ohmic heat bath. At high temperatures, we can obtain the specific heat C from (2.64). This result is exactly twice as large as the one obtained in dissipative two-state systems. As a result, the specific heat is proportional to T^{2K-2} for $0 < K < 3/2$, and proportional to T for $K > 3/2$. For details of the calculation and result, see ref. 26.

Next, we focus on the weak damping region $K \ll 1$. From eqs.(2.69)-(2.72), we obtain

$$Z = \int_0^{2\pi} \frac{d\theta}{2\pi} e^{U(n)}, \quad (3.6)$$

$$U(n) = n + \log \Gamma(Kn + 1) - Kn\psi(Kn + 1), \quad (3.7)$$

$$Q(n) = K(\psi(Kn + 1) + \bar{\gamma}), \quad (3.8)$$

$$2\beta\bar{\Delta} \cos \theta = ne^{-Q(n)}, \quad (3.9)$$

where $\bar{\gamma}$ is the Euler's constant, and $\psi(z)$ is the polygamma function. From this expression, the specific heat is obtained as Fig. 4 by numerical integration. We can see that, even for the weak damping, the specific heat is suppressed at low temperatures, and goes to zero in the limit $T \rightarrow 0$. This behavior is different from the dissipationless case $K = 0$, where C approaches a nonzero constant value at low temperatures. This result can be interpreted as follows. In the dissipationless case, the partition function is classical in the momentum in the sense that the Hamiltonian is diagonalized in the momentum space. We note that the quantization of the momentum due to a boundary condition is not taken in this formalism so that the specific heat approaches a classical nonzero value. When damping is introduced, the Hamiltonian cannot be diagonalized

in the momentum space, and the quantum effects suppress the specific heat at low temperatures.

The asymptotic expansion of Z for $\beta(\gg 1)$ gives

$$\ln Z = 2(1 - K)\beta c\Delta_{\text{eff}} + \text{const.} + \frac{1}{24K\beta c\Delta_{\text{eff}}} + \mathcal{O}(\beta^{-2}), \quad (3.10)$$

where c is a renormalization factor defined by $c = (4\pi K e^{\bar{\gamma}})^{K/(1-K)}$, and takes $c \sim 1$ for weak damping, $K \ll 1$. Details of the derivation is given in Appendix D. From the partition function, we obtain the low-temperature behavior of the system energy E and the specific heat C as

$$E = -\frac{\partial}{\partial\beta} (\ln Z) = -2(1 - K)c\Delta_{\text{eff}} + \frac{1}{24K\beta^2 c\Delta_{\text{eff}}} + \mathcal{O}(\beta^{-3}) \quad (3.11)$$

$$C = \frac{\partial E}{\partial T} = \frac{T}{12Kc\Delta_{\text{eff}}} + \mathcal{O}(T^2), \quad (3.12)$$

We can see that the specific heat is proportional to the temperature T , and the coefficient depends on the damping strength as $C \propto T/K$.

From the partition function, the density of states $D(\omega)$ is also calculated by

$$Z(\beta) = \int_{-\delta}^{\infty} d\omega D(\omega) e^{-\beta\omega}. \quad (3.13)$$

Here, the energy is shifted in order that the ground state energy becomes zero, and the infinitesimal quantity δ is introduced for convenience. From the low-temperature behavior of the partition function

$$Z \simeq e^{1/24K\beta c\Delta_{\text{eff}}} \simeq 1 + \frac{1}{24K\beta c\Delta_{\text{eff}}} + \mathcal{O}(\beta^{-2}), \quad (3.14)$$

the low-energy form of $D(\omega)$ is obtained as

$$D(\omega) \simeq \delta(\omega) + \frac{1}{24Kc\Delta_{\text{eff}}} + \mathcal{O}(\omega), \quad (3.15)$$

For the dissipative particle, $D(\omega)$ includes the delta function, while the density of state for a free particle takes a form of ω^α at low frequency, where α is an exponent dependent on the dimension. The difference indicates that the environment influences strongly the low-energy state of the system. Similar behaviors have been shown in two-state systems, where the Shottky form of the specific heat is modified to the T -linear behavior at the low temperatures.²⁶⁾ The T -linear behavior of the specific heat is expected to be caused by the environment properties, and the delta function in $D(\omega)$ cannot be explained by the one-particle picture.

3.3 Optical conductivity

3.3.1 The limit of high temperatures and/or strong dissipation

For the ohmic damping, $S(t)$ and $R(t)$ in (2.57)-(2.58) are obtained as

$$S(t) = 2K \log \left| \frac{\beta\omega_c}{\pi} \sinh \left(\frac{\pi t}{\beta} \right) \right|, \quad (3.16)$$

$$R(t) = \pi K \text{sign}(t). \quad (3.17)$$

From (2.59), we obtain the optical conductivity $\sigma_{\text{res}}(\omega) = e^2 a^2 \text{Im}\Lambda(\omega)/\omega$ as

$$\sigma_{\text{res}}(\omega) = 2e^2 a^2 \frac{\Delta^2}{\omega_c} \left(\frac{\beta\omega_c}{2\pi} \right)^{1-2K} \frac{|\Gamma(K + i\beta\omega/2\pi)|^2 \sinh \beta\omega/2}{\Gamma(2K) \omega} \quad (3.18)$$

$$= 2e^2 a^2 \Delta_{\text{eff}} \left(\frac{\beta\Delta_{\text{eff}}}{2\pi} \right)^{1-2K} \frac{|\Gamma(K + i\beta\omega/2\pi)|^2 \sinh \beta\omega/2}{\Gamma(2K) \omega}. \quad (3.19)$$

The temperature and frequency dependences of $\sigma_{\text{res}}(\omega)$ are shown in Fig. 5. In the low-frequency side ($\omega \ll KT$), $\sigma_{\text{res}}(\omega)$ depends on the temperatures. The DC conductivity $\sigma_{DC} = \sigma_{\text{res}}(\omega \rightarrow 0)$ is calculated as

$$\sigma_{DC} = 2\pi e^2 a^2 \left(\frac{\beta\Delta_{\text{eff}}}{2\pi} \right)^{2-2K} \frac{\Gamma(K)^2}{\Gamma(2K)}, \quad (3.20)$$

Fig. 5. The optical conductivity $\sigma_{\text{res}}(\omega)$ at high temperatures ($T = 6\Delta_{\text{eff}}, 12\Delta_{\text{eff}}, 18\Delta_{\text{eff}}$) for $K = 0.5$. The dashed gray line represents the asymptotic behavior ($\propto 1/\omega$) at $\omega/\Delta_{\text{eff}} \gg 1$. The characteristic energy at which the optical conductivity deviates from the asymptotic form is estimated as KT .

which is proportional to T^{2K-2} . On the other hand, in the high-frequency limit, $\sigma_{\text{res}}(\omega)$ takes a temperature-independent form

$$\sigma_{\text{res}}(\omega) = \frac{2\pi e^2 a^2}{\Gamma(2K)} \left(\frac{\Delta_{\text{eff}}}{\omega} \right)^{2-2K}. \quad (3.21)$$

On the high-frequency side, $\sigma_{\text{res}}(\omega)$ is proportional to ω^{-2+2K} , and deviates from the Drude form (3.4).

3.3.2 Weak coupling region

Next, we consider the weak damping region, $K \ll 1$. For the ohmic damping, the screened potential defined by (2.73) is calculated as

$$\varphi(\tau; \theta) = \frac{1}{\beta} \sum_{\omega_m} \frac{-2\pi K}{|\omega_m| + \gamma(\theta)} e^{i\omega_m \tau}, \quad (3.22)$$

where $\gamma = \gamma(\theta)$ is a inverse of a screening length given by

$$\gamma(\theta) = 2\pi K n(\theta) / \beta. \quad (3.23)$$

Following the usual way, the sum over the Matsubara frequency in (3.22) is replaced by an integral form. As a result, $\varphi(it; \theta) = S(t; \theta) + iR(t; \theta)$ is obtained as

$$R(t; \theta) = \pi K e^{-\gamma(\theta)t} \quad (3.24)$$

$$S(t; \theta) = 2K \int_0^\infty d\omega \frac{\omega}{\omega^2 + \gamma(\theta)^2} \left[\frac{2}{\beta\omega} - \coth \frac{\beta\omega}{2} \cos \omega t \right] + 2\pi K \Theta(-\gamma) \left[\frac{2}{\beta\omega} - \coth \frac{\beta\omega}{2} \cos \omega t \right], \quad (3.25)$$

where $\Theta(x)$ is a step function. For no damping case $\gamma \rightarrow 0$, the above expressions become unscreened potentials, $S(t)$ and $R(t)$ in (2.57)-(2.58). Analytical expressions for $S(t; \theta)$ are obtained only for two limiting cases. At high temperatures $\beta \rightarrow 0$, $S(t; \theta)$ is calculated as

$$S(t; \theta) = \frac{2\pi K}{\beta\gamma(\theta)} (1 - e^{-\gamma(\theta)t}). \quad (3.26)$$

On the other hand, at low temperatures, $S(t; \theta)$ is expanded by the temperature $T = 1/\beta$ as

$$S(t; \theta) = S_0(t; \theta) + \frac{2\pi KT}{\gamma(\theta)} + \mathcal{O}(T^2), \quad (3.27)$$

Fig. 6. The optical conductivity $\sigma(\omega)$ at zero temperature for weak damping ($K = 0, 0.1, 0.2$). As the damping increases, $\sigma(\omega)$ deviates from the Drude form ($K = 0$). At high frequency, $\sigma(\omega)$ is proportional to ω^{2K-2} .

$$S_0(t; \theta) = K \left[e^{\gamma(\theta)t} \text{Ei}(-\gamma(\theta)t) + e^{-\gamma(\theta)t} \text{Ei}(\gamma(\theta)t) \right], \quad (3.28)$$

where $\text{Ei}(z)$ is the exponential integral function, and $S_0(t)$ is a temperature-independent part. In both cases, the limiting value at $t \rightarrow \infty$ is given by

$$S(t \rightarrow \infty; \theta) = \frac{2\pi K T}{\gamma(\theta)}. \quad (3.29)$$

For all temperatures, we can calculate $\sigma(\omega)$ by the expressions (3.24)-(3.25). The calculation is, however, rather difficult. Hence, we only consider the optical conductivity at zero temperature, where the dominant contribution comes from $\theta = 0$ in the integral (2.78). The real-time correlation function for $K \ll 1$ is obtained by using the asymptotic form $n = 2\beta c \Delta_{\text{eff}}$ as

$$\Lambda(t) = \frac{\gamma_0}{2\pi K} \int_0^\infty dt e^{i\omega t - \gamma_0 t} \cosh[S_0(t)]. \quad (3.30)$$

Here, $\gamma_0 = \gamma(\theta = 0)$ is the damping frequency at $T = 0$ given by

$$\gamma_0 = 4\pi K c \Delta_{\text{eff}}, \quad (3.31)$$

where $c = (4\pi K e^{\bar{\gamma}})^{K/(1-K)}$. The optical conductivity can be calculated by numerical Fourier transformation of (3.30). The result for $\sigma_{\text{res}}(\omega)$ is shown in Fig. 6. The Drude formula (3.4) in the continuum limit is also shown. At the high frequency side, the optical conductivity of the dissipative system deviates from the Drude form.

The qualitative behavior of $\sigma(\omega)$ is obtained by considering the limiting form of $S_0(t)$:

$$S_0(t) = \begin{cases} 2K \log(e^{\bar{\gamma}} \gamma_0 t) & (t \rightarrow 0), \\ \frac{2K}{(\gamma_0 t)^2} & (t \rightarrow \infty), \end{cases} \quad (3.32)$$

where $\bar{\gamma}$ is the Euler's constant. From (3.30) and (3.32), the limiting behavior of the optical conductivity is obtained as

$$\sigma(\omega) = \begin{cases} \frac{2\pi e^2 a^2}{\Gamma(2K)} \left(\frac{\Delta_{\text{eff}}}{\omega} \right)^{2-2K}, & (\omega \gg \omega^*) \\ \frac{e^2 a^2}{2\pi K} \frac{\gamma_0^2}{\gamma_0^2 + \omega^2} & (\omega \ll \omega^*), \end{cases} \quad (3.33)$$

where $\omega^* = (2c)^{1/2K}$ is the crossover frequency at which the two expressions take the same value. The high-frequency behavior of $\sigma(\omega)$ agrees with the result of the high temperature limit (3.21). This indicates

that the high-frequency side is independent of the temperature at *any* damping strength, since (3.21) is valid at any value of K . On the other hand, the low-frequency side coincide with the Drude form (3.4) obtained in the continuum limit. It is interesting that for $K \rightarrow 0$, the asymptotic form in the limit $\omega \rightarrow \infty$ of the Drude form deviates from the high frequency form shown in the lower equation of (3.33) by factor 2. At first glance, one might have suspicion on this difference. However, this difference indeed exists: When we take the limit $K \rightarrow 0$, the crossover frequency ω^* in (3.33) goes to infinity. Then, the region $\omega \gg \omega^*$ disappears and the lower expression in (3.33) governs even the high-frequency region, which reproduces (3.4).

On the high frequency side $\omega \gg \omega^*$, the particle moves by using the heat-bath excitations. Therefore, the particle moves incoherently even at zero temperature. The results are relevant to the X-ray absorption anomaly.^{8,29)}

3.3.3 DC conductivity

We consider the DC conductivity σ_{DC} of the lattice model for the weak coupling region ($K \ll 1$). The low-temperature behavior is obtained by the asymptotic expansion over $\beta = 1/T$ as

$$\sigma_{\text{DC}}/\sigma_{\text{DC}}^0 = 1 - \frac{1}{8} \left(\frac{T}{c\Delta_{\text{eff}}} \right)^2 + \mathcal{O}(T^3), \quad (3.34)$$

where $\sigma_{\text{DC}}^0 = e^2 a^2 / 2\pi K$. (See Appendix D.) Thus, the thermal fluctuation suppresses σ_{DC} . The T^2 -suppression at low temperatures is consistent to the general study of the linear mobility $\mu_l = \sigma_{\text{DC}}/e^2$.²⁵⁾ In the previous work, the linear mobility has not been obtained correctly even in the weak damping $K \ll 1$.⁴²⁾ The high-temperature limit of σ_{DC} for $K \ll 1$ is obtained from (3.20) as

$$\sigma_{\text{DC}}/\sigma_{\text{DC}}^0 = 8\pi^2 \left(\frac{\beta\Delta_{\text{eff}}}{2\pi} \right)^{2-2K}. \quad (3.35)$$

We compare this result with the linear mobility μ_l obtained in ref. 25. For the special value $K = 1/2$, the linear mobility is calculated for all temperatures as

$$\mu_l = \frac{\mu_0 \Delta_{\text{eff}}}{2T} \psi'(\Delta_{\text{eff}}/2T + 1/2), \quad (3.36)$$

where $\psi'(z)$ is the trigamma function, and $\mu_0 = a^2/2\pi K$. At low temperatures, the DC conductivity $\sigma_{\text{DC}} = \mu_l/e^2$ behaves as

$$\sigma_{\text{DC}}/\sigma_{\text{DC}}^0 \simeq 1 - \frac{T^2}{3\Delta_{\text{eff}}^2}, \quad (3.37)$$

and show the T^2 -suppression. This strongly indicates that the T^2 -suppression appears for any value of $0 < K \leq 1/2$. The coefficient of T^2 is smaller than in (3.34). At high temperatures, the DC conductivity for $K = 1/2$ shows a $1/T$ behavior as

$$\sigma_{\text{DC}}/\sigma_{\text{DC}}^0 \simeq \frac{\pi^2 \Delta_{\text{eff}}}{4T}, \quad (3.38)$$

which agrees with (3.20) for $K = 1/2$.

3.4 One-particle Green's function

We consider one-particle Green's function in the weak damping region at zero temperature. We obtain the asymptotic expansion of the formulation (2.84) as

$$\tilde{G}_{i,i+L}(\tau) \sim -\exp \left[-KL^2 \left(\log \frac{\omega_c}{\gamma_0} + \bar{\gamma} \right) \right] \quad (3.39)$$

For details of the derivation, see Appendix D. Hence, in the limit $\omega_c/\gamma_0 \rightarrow \infty$, the one-particle Green's function $\tilde{G}_{i,i+L}(\tau)$ vanishes except for $L = 0$, and is written by

$$\tilde{G}_{i,j}(\tau) = \tilde{G}_{i,i}(\tau) \delta_{ij}. \quad (3.40)$$

Thus, the Green's function of the dissipative particle is completely local. In other words, the Fourier transformation of the Green's function

$$\tilde{G}(k, \tau) = \sum_L \tilde{G}_{i,i+L}(\tau) e^{ikL} \quad (3.41)$$

becomes independent of k . This behavior indicates that the ‘coherent’ motion of the particle is strongly suppressed even at zero temperature. The term ‘coherent’ used in this subsection means that the quasiparticle excitation is good descriptions for considered systems. In the present system, it is expected that the eigenstate of the momentum cannot be a good quantum number. This result is consistent with the study of the Brownian motion, where the expectation value $\langle p^2 \rangle$ diverges logarithmically in the limit $\omega_c/\gamma \rightarrow \infty$.²⁰⁾

The local Green’s function $\tilde{G}_{i,i}(\tau)$ have been obtained also in the retracable path approximation for correlated electron systems.^{43, 44, 45)} In this approximation, the coherent motion of the particle is strongly suppressed by the antiferromagnetic background. This mechanism is similar to the present model of the dissipative particle, when the heat bath is regarded as the antiferromagnetic background. The similarity is, however, not complete, since the density of states, $D(\omega)$ for the ohmic case given in (3.15) differs from the result obtained by the retracable path approximation. Nevertheless, we speculate that the lattice model of the dissipative particle may be utilized as a basic model of the decoherence of the particle due to the electron-electron correlation. One of the relevant problems may be the transport of a coupled Luttinger liquid.⁹⁾ The application of the Caldeira-Leggett model for correlated electrons remains for future studies.

§4. Summary

We have studied the thermodynamics and transport properties of the dissipative particle in the tight-binding model. By utilizing the imaginary-time path integral, the specific heat, the optical conductivity and one-particle Green’s function have been formulated for arbitrary form of the spectral density. A systematic approximation has been considered to treat the weak-coupling region at all temperatures. We have obtained an analytical form which can connect the high-temperature to low-temperature region.

The actual calculation has been performed for the ohmic damping case. The specific heat at weak damping shows T -linear behaviors at low temperatures. Further, one-particle Green’s function becomes completely local for the ohmic damping case in the limit $\omega_c \rightarrow \infty$ at zero temperature. These results indicate that the particle motion is always ‘incoherent’ in the sense that description by the eigenstates of momenta cannot be a good description. The optical conductivity shows non-Drude form even at zero temperature, and behaves as ω^{2K-2} on the high-frequency side, where K is the dimensionless damping strength. At high temperatures, the high-frequency side does not change the non-Drude form, and only the low-frequency side depends on the temperature T . Particularly, the DC conductivity is proportional to T^{2K-2} .

In this paper, we have focused only on the ohmic damping. The detailed calculation for the non-ohmic damping and the solvable line $K = 1/2$ remains for future study. We speculate that the treatment of the Caldeira-Leggett theory in the lattice system may be used for basic descriptions of the incoherent transport in correlated electron systems. Further application with a self-consistent treatment and the effectiveness also remains for further study.

Appendix A: Non-ohmic Damping in the Incoherent Tunneling Regime

In this appendix, we study the optical conductivity $\sigma(\omega)$ for the non-ohmic damping case in the incoherent regime following the formulation in § 2.5. The results on the tunneling rate $\Gamma(\varepsilon)$ obtained in ref. 14 are utilized to obtain $\sigma(\omega)$. We only consider a few limiting cases which allow analytical treatment.

We begin with the superohmic damping $1 < s < 2$. Under the strong bias $\varepsilon \gg \bar{\Delta}$ and the weak coupling condition $\delta_s(\varepsilon/\tilde{\omega})^{s-1} \ll 1$, the tunneling rate $\Gamma(\varepsilon)$ is calculated as

$$\Gamma(\varepsilon) = \frac{a^2}{2} \left(\frac{2\bar{\Delta}}{\varepsilon} \right)^2 J(\varepsilon) \coth(\beta\omega/2). \quad (\text{A}\cdot 1)$$

By using (1.5) and (2.63), we obtain the optical conductivity as

$$\sigma(\omega) = 4\pi\delta_s \left(\frac{\bar{\Delta}}{\omega} \right)^2 \left(\frac{\omega}{\tilde{\omega}} \right)^{s-1}, \quad (\text{A}\cdot 2)$$

which is temperature-independent at all temperatures. Hence, the optical conductivity behaves as $\sigma(\omega) \propto \omega^{s-3}$. This behavior corresponds to the result (2.53) in the continuum limit ($T, \delta_s \rightarrow 0$) on the high frequency side, except a difference by a factor 2. Similar difference appears also in the case of the ohmic damping, and the origin of the factor 2 is expected to be the same. (See (3.33) and the following text.)

The tunneling rate for $\varepsilon = 0$ is calculated as follows:

$$\Gamma = \left(\frac{(2-s)\sin(\pi s/2)}{2\delta_s\Gamma(s-1)\sin\pi(s-1)} \right)^{1/(2-s)} \Gamma\left(\frac{3-s}{2-s}\right) \frac{\bar{\Delta}^2}{\tilde{\omega}} \left(\frac{\tilde{\omega}}{T}\right)^{1/(2-s)}. \quad (\text{A}\cdot 3)$$

This result is valid at high temperatures $T^* \ll T (\ll \omega_c)$, where T^* is given by

$$T^* = \frac{\bar{\Delta}}{\delta_s\Gamma(s-1)} \left(\frac{\tilde{\omega}}{\bar{\Delta}}\right)^{s-1}. \quad (\text{A}\cdot 4)$$

The DC conductivity is obtained from (A·3) by $\sigma_{\text{DC}} = e^2 a^2 \Gamma / 2T$, and behaves as $\sigma_{\text{DC}} \propto T^{-\frac{3-s}{2-s}}$ at high temperatures. The exponent of T decreases from -2 to $-\infty$ as increasing s from 1 to 2.

Next, we consider the subohmic damping $0 < s < 1$. At zero temperature, the tunneling rate is calculated under the condition $\delta_s(\varepsilon/\tilde{\omega})^{s-1} \gg 1$ as

$$\begin{aligned} \Gamma(\varepsilon) &= \frac{(B\Delta)^2}{4\tilde{\omega}} \left(\frac{2\pi[2\delta_s\Gamma(s)]^{1/2}}{s} \right)^{1/2} \left(\frac{\tilde{\omega}}{\varepsilon} \right)^{(1+s)/2s} \\ &\times \exp \left[-\frac{s}{1-s} [2\delta_s\Gamma(s)]^{1/s} \left(\frac{\tilde{\omega}}{\varepsilon} \right)^{(1-s)/s} \right], \end{aligned} \quad (\text{A}\cdot 5)$$

where $B = \exp[\delta_s|\Gamma(s-1)|(\tilde{\omega}/\omega_c)^{1-s}]$. This result cannot be related to the result of the continuum limit because of the strong coupling condition $\delta_s(\varepsilon/\tilde{\omega})^{s-1} \gg 1$. The optical conductivity is obtained by $\sigma(\omega) = a^2 e^2 \Gamma(\varepsilon)/\varepsilon$, and behaves as $\sigma(\omega) \sim \varepsilon^{-(1+3s)/2s} \exp(-\text{const.}\varepsilon^{-(1-s)/s})$. Notice that the optical conductivity vanishes with an essential singularity as $\varepsilon \rightarrow 0$.

The tunneling rate for $\varepsilon = 0$ for the condition $\delta_s(\tilde{\omega}/T)^{1-s} \gg 1$ is given by

$$\begin{aligned} \Gamma &= \frac{(B\Delta)^2}{2\tilde{\omega}} \left(\frac{\tilde{\omega}}{T} \right)^{(1+s)/2} \left(\frac{\pi}{2(1+s)^2\Gamma(s)\zeta(1+s)\delta_s} \right)^{1/2} \\ &\times \exp \left[-\frac{1+s}{1-s} \Gamma(s) \left(\frac{1}{2(1+s)\zeta(1+s)} \right)^{(1-s)/(1+s)} \delta_s \left(\frac{\tilde{\omega}}{T} \right)^{1-s} \right]. \end{aligned} \quad (\text{A}\cdot 6)$$

From (A·6), the DC conductivity is obtained by $\omega_{\text{DC}} = a^2 e^2 \Gamma / 2T$, and behaves as $\omega_{\text{DC}} \sim T^{-(1+3s)/2s} \exp(-\text{const.} \times T^{-(1-s)/s})$. The DC conductivity vanishes with an essential singularity as $T \rightarrow 0$, and this result is consistent with the continuum limit, where $\sigma_{\text{reg}}(\omega \rightarrow 0) = 0$. Note that the power law $\sigma_{\text{DC}} \sim T^{2K-2}$ for the ohmic case $s = 1$ is obtained from (A·6) by carefully considering the limit $s \rightarrow 1^-$.

Appendix B: Calculation of ϕ_0

In this appendix, we evaluate the zero frequency component $\phi_0 = \phi(i\omega_m = 0)$. From (2.65) and (2.3)-(2.4), ϕ_0 is explicitly given as

$$\phi_0 = \frac{a^2}{\pi} \int_0^\infty d\omega \frac{J(\omega)}{\omega^2} \left(\coth \frac{\beta\omega}{2} - \frac{2}{\beta\omega} \right). \quad (\text{B}\cdot 1)$$

We consider the analytical form of the spectral density,

$$J(\omega) = \frac{2\pi\delta_s}{a^2} \left(\frac{\omega}{\tilde{\omega}} \right)^{s-1} \omega e^{-\omega/\omega_c}, \quad (\text{B}\cdot 2)$$

where the exponential cut-off is adopted, and the cutoff frequency ω_c is taken as $\Delta, 1/\beta \ll \omega_c$. By substituting (B·2) to (B·1), we obtain

$$\phi_0 = 2\delta_s \left(\frac{\omega_c}{\tilde{\omega}} \right)^z \Gamma(z) \left[\frac{2}{(\beta\omega_c)^z} \zeta(z, 1/\beta\omega_c) - 1 - \frac{2}{z-1} \frac{1}{\beta\omega_c} \right] \quad (\text{B}\cdot 3)$$

$$\simeq 2\delta_s \left(\frac{\omega_c}{\tilde{\omega}} \right)^z \Gamma(z) \left[1 + \frac{2\zeta(z)}{(\beta\omega_c)^z} + \mathcal{O}(1/\beta\omega_c) \right], \quad (\text{B}\cdot 4)$$

where $z = s - 1$, and $\zeta(z, a)$ is the generalized zeta function, and $\zeta(z)$ is the zeta function. In the second equation, we have left only the leading terms under the condition $\beta\omega_c \gg 1$. For superohmic case $z > 0$, the first term in the bracket is dominant, and ϕ_0 is independent of temperatures. Further, the result is expressed

generally reproduced by the Frank-Condon factor calculated as

$$\phi_0 = \frac{a^2}{\pi} \int_0^\infty \frac{J(\omega)}{\omega^2} d\omega, \quad (\text{B}\cdot 5)$$

when the integral is convergent as in the case of the superohmic damping $s > 1$. On the other hand, for subohmic damping $z = s - 1 < 0$, the second term in the bracket in (B·4) is dominant. Hence, ϕ_0 depends on temperatures. For the ohmic case $s = 1$, the expression (B·4) fails, and careful treatment of (B·3) is required. As a result, the leading term in ϕ_0 depends logarithmically on temperatures as

$$\phi_0 \simeq 2K \log \frac{\beta\omega_c}{2\pi}, \quad (\text{B}\cdot 6)$$

where $K = \delta_1$. In this case, the renormalized matrix element (2.68) is given by

$$\bar{\Delta} = \Delta \left(\frac{\beta\omega_c}{2\pi} \right)^{-K}. \quad (\text{B}\cdot 7)$$

At a first glance, one might regard that this result is unphysical, because the matrix element is reduced to zero as the temperature decreases even for the weak coupling region $K \ll 1$. We, however, show that the renormalization factor $(\beta\omega_c/2\pi)^{-K}$ is canceled by other factors for observables in the weak coupling theory.

Appendix C: Ring Approximation

In this appendix, we give details of the calculation in the weak coupling theory (§ 2.6) for the arbitrary form of $J(\omega)$. We first study the partition function based on the cluster expansion of classical imperfect gas.⁴⁶⁾ The partition function, optical conductivity and one-particle Green's function are also formulated by the ring approximation.

We begin with the partition function (2.12). After the potential shift (2.67), we obtain

$$Z = \sum_{m=0}^{\infty} \frac{\bar{\Delta}^{2m}}{m!m!} \prod_{l=1}^m \int_0^\beta d\tau_l \int_0^\beta d\rho_l \times \exp \left[\sum_{k<l}^m \{ \phi(\tau_l - \tau_k) + \phi(\rho_l - \rho_k) \} - \sum_{l=1}^m \sum_{k=1}^m \phi(\tau_l - \rho_k) \right], \quad (\text{C}\cdot 1)$$

where $\bar{\Delta}$ is a renormalized transition amplitude defined by (2.68). Here, new integral variables, $\{\tau_l\}$ and $\{\rho_l\}$ describe the positions of positive ($\xi_l = +1$) and negative ($\xi_l = -1$) charges. Note that the partition function is multiplied by the factor $2m!/m!m!$. This factor comes from the number of the ways in which $2m$ charges are divided into two groups consisting of m charges to guarantee the electroneutrality condition (2.13). Then, we consider the cluster expansion for the partition function (C·1). To simplify the expansion, we rewrite it as the following form

$$Z = \sum_{m=0}^{\infty} \frac{(\beta\bar{\Delta})^{2m}}{m!m!} \left\langle \prod_{k<l}^m (1 + f_{kl}^{++})(1 + f_{kl}^{--}) \prod_{k=1}^m \prod_{l=1}^m (1 + f_{kl}^{+-}) \right\rangle. \quad (\text{C}\cdot 2)$$

Here, the potential $\phi(\tau)$ is replaced by Mayer's functions

$$f_{kl}^{++} = e^{\phi(\tau_k - \tau_l)} - 1, \quad (\text{C}\cdot 3)$$

$$f_{kl}^{--} = e^{\phi(\rho_k - \rho_l)} - 1, \quad (\text{C}\cdot 4)$$

$$f_{kl}^{+-} = e^{-\phi(\tau_k - \rho_l)} - 1, \quad (\text{C}\cdot 5)$$

and $\langle \dots \rangle$ denotes the average

$$\langle \dots \rangle = \frac{1}{\beta^{2m}} \prod_{l=1}^m \int_0^\beta d\tau_l \int_0^\beta d\rho_l (\dots). \quad (\text{C}\cdot 6)$$

Each term in the expansion on f_{kl} in (C·2) is expressed by a product of integrals of clusters. We introduce

Fig. 7. The diagrams representing the integrals $b_{l,m}$ in (C·8)-(C·12). The closed (open) circles denotes the positive (negative) charges. Note that $b_{l,m} = b_{m,l}$.

cluster integrals

$$b_{l,k} = \frac{1}{l!k!} \sum_{\text{clusters}} \langle \prod_{i,j} f_{ij}^{\sigma_i \sigma_j} \rangle, \quad (\text{C}\cdot 7)$$

where \sum_{clusters} denotes the sum of all clusters including k positive charges and l negative charges. The products are taken over all bonds combining i -th and j -th charges in each cluster, where σ_i and σ_j are signs of charges. For example, the explicit form of $b_{l,k}$ for small k, l is given by

$$b_{0,0} = 0, \quad b_{10} = b_{01} = 1, \quad (\text{C}\cdot 8)$$

$$b_{2,0} = \frac{1}{2} \langle f_{12}^{++} \rangle, \quad (\text{C}\cdot 9)$$

$$b_{1,1} = \langle f_{12}^{+-} \rangle, \quad (\text{C}\cdot 10)$$

$$b_{3,0} = \frac{1}{6} \langle f_{12}^{++} f_{23}^{++} f_{31}^{++} + 3f_{12}^{++} f_{23}^{++} \rangle, \quad (\text{C}\cdot 11)$$

$$b_{2,1} = \frac{1}{2} \langle f_{12}^{++} f_{23}^{+-} f_{13}^{+-} + 2f_{12}^{++} f_{23}^{+-} + f_{13}^{+-} f_{23}^{+-} \rangle, \quad (\text{C}\cdot 12)$$

and so on. The above integrals can be viewed by graphical representations as shown in Fig. 7. By the cluster integrals $b_{l,k}$, the partition function is expressed as

$$\begin{aligned} Z &= \sum_{m=0}^{\infty} \frac{(\beta\bar{\Delta})^{2m}}{m!m!} \sum_{\{m_{l,k}\}'} \frac{m!}{\prod_{l,k} m_{l,k}! (l!)^{m_{l,k}}} \\ &\times \frac{m!}{\prod_{l,k} m_{l,k}! (k!)^{m_{l,k}}} \times \prod_{l,k} (l!k! b_{l,k})^{m_{l,k}} \times \prod_{l,k} m_{l,k}!, \end{aligned} \quad (\text{C}\cdot 13)$$

where $m_{l,k}$ is the number of clusters including l positive charges and k negative charges. The sums and products are taken over l and k except for the case $(l,k) = (0,0)$. The prime in $\{m_{l,k}\}'$ denotes the summation in accordance with the conditions

$$\sum_{l,k} l m_{l,k} = m, \quad (\text{C}\cdot 14)$$

$$\sum_{l,k} k m_{l,k} = m. \quad (\text{C}\cdot 15)$$

The first (second) factor in the sum $\sum_{\{m_{l,k}\}'}$ in (C·13) gives the number of ways in which m positive (negative) charges can be distributed into the clusters. The third part is the relevant cluster integrals, and the fourth part is the number of ways to combine $m_{l,k}$ groups of positive charges to $m_{l,k}$ groups of negative charges.

Fig. 8. The diagrammatic graphs representing the expansion in (C·21) and (C·22) are drawn in (a). The graphs in both (b) and (c) are representative cluster integrals: (b) each charge has even bonds, while (c) includes charges with odd bonds.

From (C·14)-(C·15), we obtain the constraint on the total number of charges as

$$\sum_{l,k} (l+k)m_{l,k} = 2m, \quad (\text{C·16})$$

and this constraint can be removed by the sum over m . On the other hand, the electroneutrality condition

$$\sum_{l,k} (l-k)m_{l,k} = 0, \quad (\text{C·17})$$

remains. To remove the constraint (C·17), we introduce an integral over a new variable θ as

$$\sum_{m=0}^{\infty} \sum_{\{m_{l,k}\}'} (\dots) = \sum_{\{m_{l,k}\}} \int_0^{2\pi} \frac{d\theta}{2\pi} \exp\left(i \sum_{l,k} (l-k)m_{l,k}\theta\right) (\dots). \quad (\text{C·18})$$

Thus, the partition function Z is obtained as

$$Z = \int_0^{2\pi} \frac{d\theta}{2\pi} \exp\left(\sum_{l,k} b_{l,k}(\beta\bar{\Delta})^{l+k} e^{i(l-k)\theta}\right). \quad (\text{C·19})$$

For the dissipationless case ($K = 0, \bar{\Delta} = \Delta$), $b_{l,k}$ vanishes for $l+k \geq 2$ and the partition function is exactly calculated as

$$Z = \int_0^{2\pi} \frac{d\theta}{2\pi} \exp(2\beta\Delta \cos \theta) = I_0(2\beta\Delta), \quad (\text{C·20})$$

where $I_0(z)$ is the Modified Bessel function. Of course, this result is also obtained by usual treatment for the tight-binding model of a free particle.

So far, the obtained expression for Z is exact. In the following discussion, the so-called ‘ring approximation’ is introduced. First, we expand $f_{ij}^{\sigma_i\sigma_j}$ as

$$f_{ij}^{++} = f_{ij}^{--} = \sum_{n=1}^{\infty} \frac{\{\phi(\tau_i - \tau_j)\}^n}{n!}, \quad (\text{C·21})$$

$$f_{ij}^{+-} = \sum_{n=1}^{\infty} \frac{\{-\phi(\tau_i - \tau_j)\}^n}{n!}. \quad (\text{C·22})$$

Graphical representations of the expansion is given in Fig. 8(a), where the bond denoted with n thin lines denotes $\phi(\tau_i - \tau_j)^n$. Here, we assume that (I) the dominant contribution comes from the clusters in which each charge is combined by ‘even’ bonds to other charges. Based on the assumption (I), we neglect other clusters which do not satisfy this condition. For example, we consider the graphs as shown in Fig. 8(b), and neglect the graphs as shown in Fig. 8(c). The assumption (I) is justified in the ring approximation denoted

later in detail. At this stage, however, in order to avoid confusion, we do not justify the assumption (I). We mention this point after introducing the ring approximation.

The diagrams as shown in Fig. 8(b) have a crucial property that the cluster integral on the graphs remains constant when the sign of each charge is reversed. As a result, the cluster integral $l!k!b_{l,k}$ depends only on the total charge number $l+k$. In this situation, $l!k!b_{l,k}$ can be denoted with $(l+k)!b_{l+k}$, and the sum over l, k under the constraint $l+k=m$ in the partition function (C.19) gives

$$Z = \int_0^{2\pi} \frac{d\theta}{2\pi} \exp\left(\sum_{m=1}^{\infty} b_m \xi^m\right). \quad (\text{C}\cdot 23)$$

Here $\xi = 2\beta\bar{\Delta} \cos\theta$ is regarded as a fugacity of ‘one-component’ classical charges. Because the remaining calculation follows the usual procedure of the classical imperfect gas as given in ref. 46, we briefly note the results. The diagrams, in which all charges are more than singly connected, are called irreducible diagrams. The irreducible integrals β_l are defined on the irreducible diagrams with the size $(l+1)$ as

$$\beta_l = \frac{1}{l!} \sum_{\substack{\text{irreducible} \\ \text{clusters}}} \langle \prod_{i,j} (\sigma_i \sigma_j \phi_{ij})^{n_{i,j}} \rangle, \quad (\text{C}\cdot 24)$$

where the product is taken over all bonds in a cluster, and $n_{i,j}$ is the number of bonds combining i -th and j -th charges. Every cluster integral b_l can be expressed as a sum of terms, each of which is a numerical coefficient multiplied by a product of powers of the reduced integrals β_l as

$$\begin{aligned} b_1 &= 1, & b_3 &= \frac{1}{2}\beta_1^2 + \frac{1}{3}\beta_2, \\ b_2 &= \frac{1}{2}\beta_1, & b_4 &= \frac{2}{3}\beta_1^3 + \beta_1\beta_2 + \frac{1}{4}\beta_3. \end{aligned} \quad (\text{C}\cdot 25)$$

In general, it is proved that the equation for b_l is

$$b_l = \frac{1}{l^2} \sum_{\{m_k\}'} \prod_k \frac{(l\beta_k)^{m_k}}{m_k!}, \quad (\text{C}\cdot 26)$$

where the prime in $\{m_k\}'$ denotes the summation subject to the constraint

$$\sum_{k=1}^{l-1} km_k = l-1. \quad (\text{C}\cdot 27)$$

We also define a particle density n by

$$n = \sum_{m=1}^{\infty} mb_m \xi^m. \quad (\text{C}\cdot 28)$$

This value corresponds to the average of the hopping number in the imaginary-time path $q(\tau)$ in the original action, and qualitatively gives an effective hopping amplitude through $\Delta_{\text{eff}}^{-1} \simeq \beta/n$. By using β_l and n , the partition function Z can be expressed in a closed form. To see this, we expand ξ by n as

$$\xi = a_1 n + a_2 n^2 + \dots, \quad (\text{C}\cdot 29)$$

and determine a_1, a_2, \dots so that (C.28) is satisfied. Thus, we obtain

$$\begin{aligned} a_1 &= b_1^{-1} = 1, & a_3 &= 8b_2^2 - 3b_3, \\ a_2 &= -2b_2, & a_4 &= -40b_2^3 + 30b_2b_3 - 4b_4. \end{aligned} \quad (\text{C}\cdot 30)$$

From (C.25), these results can be rewritten in terms of the β_l 's as

$$\begin{aligned} a_1 &= 1, & a_3 &= -(\beta_2 - \frac{1}{2}\beta_1^2), \\ a_2 &= -\beta_1, & a_4 &= -(\beta_3 - \beta_1\beta_2 + \frac{1}{6}\beta_1^3). \end{aligned} \quad (\text{C}\cdot 31)$$

In general, ξ is expressed by the particle density n as

$$\xi = 2\beta\bar{\Delta} \cos\theta = n \exp\left(-\sum_{l=1}^{\infty} \beta_l n^l\right). \quad (\text{C}\cdot 32)$$

It can be easily checked that the first four terms in expansion of (C.32) gives (C.31). The partition function

Fig. 9. The ring irreducible graphs considered in the ring approximation.

(C·23) is expressed in terms of β_l and n by utilizing (C·29) and (C·31). As a result we obtain

$$Z = \int_0^{2\pi} \frac{d\theta}{2\pi} \exp[U(n)], \quad (\text{C}\cdot\text{33})$$

$$U(n) = n \left(1 - \sum_{l=1}^{\infty} \frac{l}{l+1} \beta_l n^l \right). \quad (\text{C}\cdot\text{34})$$

When we introduce

$$Q = \sum_{l=1}^{\infty} \beta_l n^l, \quad (\text{C}\cdot\text{35})$$

the relation (C·32) and the exponent $U(n)$ is expressed in simple forms as

$$\xi = n e^{-Q(n)} \quad (\text{C}\cdot\text{36})$$

$$U = n + \int_0^n dn Q - nQ. \quad (\text{C}\cdot\text{37})$$

At this stage, we introduce the approximation by assuming that only the ring irreducible diagrams as shown in Fig. 9 are dominant. This approximation is called the ‘ring approximation’. Then, the irreducible integrals β_l is expressed by the Fourier component $\phi(i\omega_m)$ as

$$\beta_l = \frac{1}{2\beta^{l+1}} \sum_{i\omega_m} \phi(i\omega_m)^{l+1}, \quad (\text{C}\cdot\text{38})$$

and thus we obtain

$$Q = \frac{1}{\beta^2} \sum_{\omega_m > 0} \frac{n\phi(i\omega_m)^2}{1 - n\phi(i\omega_m)/\beta}. \quad (\text{C}\cdot\text{39})$$

Here, the sum is taken over the Matsubara frequency, $\omega_m = 2\pi m/\beta$. The justification of the ring approximation is not clear. It, however, can be proved that this approximation is equivalent to the Debye-Hückel theory, which has been considered to calculate thermodynamic quantities in strong electrolytes.⁴⁷⁾ In the Debye-Hückel theory, the screening effects due to the other charges are described by a screening potential $\varphi(\tau)$. (The explicit form of the screening potential is given in (2.73).) These screening effects are essential to study thermodynamic quantities at low-temperatures in the original model. In the ring approximation, the assumption (I) adopted in the previous discussion is automatically satisfied, because the neglected diagrams by the assumption (I) are also removed in the ring approximation.

We study the condition, in which the ring approximation is justified. From (C·39), it is expected that the ring approximation is certainly valid as long as the expansion quantity $n\phi(\omega_m)/\beta$ is small enough at $\omega_m \sim 1/\bar{\tau}$, where $\bar{\tau} \sim \beta/n \sim \Delta_{\text{eff}}^{-1}$ is a average distance between two particles. For the exponent $0 < s < 2$ in the spectral density, this condition corresponds to

$$\delta_s \left(\frac{\Delta_{\text{eff}}}{\bar{\omega}} \right)^{s-1} \ll 1. \quad (\text{C}\cdot\text{40})$$

In the ohmic damping case ($s = 1$, $\delta_s = K$), this condition is nothing but the weak-damping condition $K \ll 1$, where we expect that the approximation gives reliable results in the weak-damping region.

Next, we calculate the optical conductivity. The correlation function $\tilde{\Lambda}_1(\tau)$ in (2.27) is expressed by the

Fig. 10. (a) The representative diagram relevant to the optical conductivity in the ring approximation. The renormalization of the fugacity ξ is denoted with the sum of diagram (b). The diagram (a) can be divided into the lines with l charges as shown in Fig. (c).

cluster integrals as

$$\begin{aligned} \tilde{\Lambda}_1(\tau) &= \frac{2\bar{\Delta}^2}{Z} \int_0^{2\pi} \frac{d\theta}{2\pi} \exp \left(\sum_{l,k} b_{l,k}(\beta\bar{\Delta})^{l+k} e^{i\theta(l-k)} \right) \\ &\times \sum_{l,k} B_{l,k}(\beta\bar{\Delta})^{l+k} e^{i\theta(l-k)}. \end{aligned} \quad (\text{C}\cdot 41)$$

Here, $B_{l,k}$ is the cluster integral of the diagram including two ‘fixed’ charges at $\tau' = 0, \tau$, and l and k are the numbers of additional positive and negative charges. Note that diagrams in which the two ‘fixed’ charges are separated into two clusters do not contribute to the optical conductivity, because such terms are independent of τ .

In the ring approximation, (C·41) is reduced to the partition function of one-component charged particles. Thus, we obtain

$$\tilde{\Lambda}_1(\tau) = \frac{1}{2\beta^2 Z} \int_0^{2\pi} \frac{d\theta}{2\pi} \frac{\xi^2}{\cos^2 \theta} \exp \left(\sum_{m=1}^{\infty} b_m \xi^m \right) \sum_{m=1}^{\infty} B_m \xi^m, \quad (\text{C}\cdot 42)$$

where $\xi = 2\beta\bar{\Delta} \cos \theta$. Since the sum of $b_m \xi^m$ gives U as shown in (C·23) and (C·33)-(C·34), the remaining problem is the sum of $B_m \xi^m$, which comes from the cluster integrals of the diagrams including two fixed charges. In the ring approximation, only the diagrams shown in Fig. 10(a) are relevant. The double circle in the diagram denotes the sum of the diagrams as shown in Fig. 10 (b), and renormalize the fugacity ξ as

$$\xi \rightarrow \xi \sum_{m=0}^{\infty} m b_m \xi^{m-1} = \xi \frac{dU}{d\xi}. \quad (\text{C}\cdot 43)$$

By using (C·34), it is proved that the renormalization is given by $\xi \rightarrow n$, where n is the particle density.

Finally, we consider the sum of the diagrams represented by Fig. 10 (a). The cluster integrals including

Fig. 11. (a) The representative diagram relevant to the Green's function in the ring approximation. The diagram can be divided into the lines as shown in Fig. (b)

two 'fixed' charges are summed up as

$$\sum_{m=0}^{\infty} B_m n^m = \sum_{m=0}^{\infty} \frac{n^m}{m!} \sum_{\{m_l\}'} \frac{m!}{\prod_{l=0}^m m_l! (l!)^{m_l}} \prod_{l=0}^m (C_l l!)^{m_l} \times (-1)^{m_l m_l!} \quad (\text{C}\cdot 44)$$

$$= \exp \left(- \sum_{l=0}^{\infty} C_l n^l \right). \quad (\text{C}\cdot 45)$$

Here, C_l denotes the sum shown in Fig. 10(c), and is obtained as

$$C_l = \frac{1}{l!} \times \frac{l!}{\beta^{l+1}} \sum_{i\omega_m} \phi(i\omega_m)^{l+1} e^{-i\omega_m \tau}. \quad (\text{C}\cdot 46)$$

From (C·42) and (C·45)-(C·46), the equation (2.75) is derived. Similarly, $\tilde{\Lambda}_2(\tau)$ is derived by removing the last term $(-1)^{m_l}$ in (C·44), and by replacing the electroneutrality condition (2.13) with (2.29).

At last, we consider the Green's function given by (2.40)-(2.41). Because the Green's function can be interpreted as the partition function of classical plasma, the procedure of the approximation is quite similar to the one for the partition function. We approximate the Green's function by assuming that each charge has even bonds. By the cluster integrals of the one-component plasma, the approximate expression of $\tilde{G}_{i,i+L}(\tau)$ is given by

$$\tilde{G}_{i,i+L}(\tau) = e^{-L^2 \phi_0/2} \int_0^{2\pi} \frac{d\theta}{2\pi} e^{-iL\theta} \exp \left[\sum_{m=0}^{\infty} b_m \xi^m \right] \sum_{m=0}^{\infty} G_m \xi^m, \quad (\text{C}\cdot 47)$$

where $\xi = 2\beta\bar{\Delta} \cos \theta$, and ϕ_0 is the potential shift given in (2.67). Here, G_m are the cluster integrals of the diagrams including a 'fixed' particle with L charge at $\tau' = 0$. Because the exponent in (C·47) gives $U(\theta)$ as shown in the calculation of the partition function, only the calculation of G_m remains. The relevant diagrams in the ring approximation are represented by Fig. 11 (a). The double circle is defined with the sum in Fig. 11 (b), and renormalizes the fugacity as $\xi \rightarrow n$. The diagram in Fig. 11 (a) is divided into the lines as shown in Fig. 11 (b), and the Green's function is expressed by

$$\tilde{G}(\tau) = e^{-L^2 \phi_0/2} \int_0^{2\pi} \frac{d\theta}{2\pi} e^{-iL\theta} \exp \left[U(\theta) + \sum_{l=1}^{\infty} H_l n^l \right], \quad (\text{C}\cdot 48)$$

where the integrals of the lines are given by

$$H_l = \frac{L^2}{l!} \times \frac{l!}{\beta^{l+1}} \sum_{i\omega_m} \phi(i\omega_m)^{l+1}. \quad (\text{C}\cdot 49)$$

Here, the factor L^2 appears in H_l , because the two bond connected to the fixed charge is L times as large as the other bonds between normal charges. From (C.46), we obtain $H_l = L^2 C_l$. Thus, we obtain (2.84).

Appendix D: Low-Temperature Expansions

In this appendix, we discuss the low-temperature expansions for a specific heat, a DC conductivity and one-particle Green's functions in the case of the ohmic damping. This expansion is obtained by asymptotic expansions in terms of the inverse temperature $\beta = 1/T$. We begin with the partition function Z expressed by

$$Z = \int_{-\pi}^{\pi} \frac{d\theta}{2\pi} e^{U(\theta)}. \quad (\text{D}\cdot 1)$$

Here, $U(\theta) = U(n(\theta))$ is given by

$$U(n) = n + \log \Gamma(Kn + 1) - Kn\varphi(Kn + 1), \quad (\text{D}\cdot 2)$$

where $\Gamma(z)$ is the gamma function, and $\varphi(z)$ is the polygamma function. At low temperatures, the integral in (D.1) is determined by the contribution around $\theta = 0$. We expand $U(\theta)$ as

$$U(\theta) \simeq U(0) + \frac{1}{2}U''(0)\theta^2 + \mathcal{O}(\theta^4), \quad (\text{D}\cdot 3)$$

and the integral (D.1) is replaced with the Gaussian integral by (D.3), approximately. By using $U''(0) = -n_0$ and asymptotic forms of $\Gamma(z)$ and $\phi(z)$, we obtain

$$Z = (1 - K)n_0 + \text{const.} + \frac{1}{6Kn_0} + \mathcal{O}(n_0^{-2}), \quad (\text{D}\cdot 4)$$

where $n_0 = n(\theta = 0)$. We should note that the asymmetry part $U'''(0)$ also gives a term of order of $1/n_0$. However, the term takes a finite value for $K \rightarrow 0$, and for weak damping ($K \ll 1$), and this contribution is less than the third term of (D.4). From (3.8) and (3.9), n_0 is determined by

$$2\beta\bar{\Delta} = n_0 e^{-Q(n_0)} \quad (\text{D}\cdot 5)$$

$$Q(n_0) = K(\phi(Kn_0 + 1) + \bar{\gamma}). \quad (\text{D}\cdot 6)$$

Next, we calculate the asymptotic form of (D.5). By using $\bar{\Delta} = \Delta(\beta\omega_c/2\pi)^{-K}$ and $\Delta_{\text{eff}} = \Delta(\Delta/\omega_c)^{K/(1-K)}$, the lefthand side of (D.5) is represented as $4\pi(\beta\Delta_{\text{eff}}/2\pi)^{1-K}$. For $\beta \rightarrow \infty$ ($n \rightarrow \infty$), the righthand side of (D.5) is expanded as

$$n_0 e^{-Q(n_0)} = (Ke^{K\bar{\gamma}})^{-K} n_0^{1-K} \left(1 - \frac{1}{2n_0} + \frac{1}{12Kn_0^2} + \mathcal{O}(n_0^{-3}) \right). \quad (\text{D}\cdot 7)$$

We substitute $n_0 = a_1\beta + a_0 + a_{-1}/\beta + \dots$ to (D.7), and determine the constants a_1, a_0, a_{-1} so that (D.7) gives the lefthand side of (D.5). Thus, we obtain

$$n_0 = 2\beta c \Delta_{\text{eff}} + \frac{1}{2(1-K)} - \frac{1}{24K\beta c \Delta_{\text{eff}}} + \mathcal{O}(\beta^{-2}), \quad (\text{D}\cdot 8)$$

where $c = (4\pi Ke^{K\bar{\gamma}})^{K/(1-K)}$. From (D.4) and (D.8), we obtain the low-temperature expansion of the partition function, (3.10).

In order to calculate σ_{DC} , it is sufficient to consider the long-time behavior of $S(t; \theta)$ and $R(t; \theta)$ defined in (3.24)-(3.25). From (3.25) and (3.29), we obtain for $t \rightarrow \infty$

$$S(t; \theta) = \frac{2\pi KT}{\gamma(\theta)} = \frac{1}{n}, \quad (\text{D}\cdot 9)$$

$$R(t; \theta) = \pi K e^{-\gamma(\theta)t}. \quad (\text{D}\cdot 10)$$

Here, we have used $\gamma(\theta) = 2\pi Kn(\theta)/\beta$. From (2.78), the real-time correlation function in the long-time limit is obtained as

$$\Lambda(t) = \frac{e^2 a^2}{Z} \int_{-\pi}^{\pi} \frac{d\theta}{2\pi} \frac{n^2}{\beta^2 \cos^2 \theta} e^{U(\theta)} \left[e^{-1/n} + e^{1/n} \cos 2\theta \right] \pi K e^{-\gamma(\theta)t}. \quad (\text{D}\cdot 11)$$

Then, the DC conductivity is calculated as

$$\begin{aligned}\sigma_{\text{DC}} &= \lim_{\omega \rightarrow 0} \frac{1}{\omega} \text{Im} \int_0^\infty dt e^{i\omega t} \Lambda(t) \\ &= \frac{\sigma_{\text{DC}}^0}{2Z} \int_{-\pi}^\pi \frac{d\theta}{2\pi} e^{U(\theta)} \left[\frac{e^{-1/n} - e^{1/n}}{\cos^2 \theta} + 2e^{1/n} \right],\end{aligned}\quad (\text{D}\cdot 12)$$

where $\sigma_{\text{DC}}^0 = e^2 a^2 / 2\pi K$. The low-temperature expansion is obtained by expanding (D.12) over $1/n (\ll 1)$ as

$$\sigma_{\text{DC}} = \frac{\sigma_{\text{DC}}^0}{Z} \int_{-\pi}^\pi \frac{d\theta}{2\pi} \left[1 + \frac{1}{2n^2} - \frac{1}{n} \theta^2 + \mathcal{O}(n^{-2}, \theta^4) \right] e^{U(0) + U''(0)\theta^2/2}.\quad (\text{D}\cdot 13)$$

By using the Gaussian integral formulas and an asymptotic form of the partition function

$$Z = \int_{-\infty}^\infty \frac{d\theta}{2\pi} e^{U(0) + U''(0)\theta^2/2},\quad (\text{D}\cdot 14)$$

we obtain

$$\sigma(\omega) = \sigma_{\text{DC}}^0 \left(1 - \frac{1}{2n^2} + \mathcal{O}(n^4) \right).\quad (\text{D}\cdot 15)$$

From (D.8) and (D.15), we obtain (3.34).

Finally, we study one-particle Green's function $\tilde{G}_{i,i+L}(\tau)$ in the low-temperature region. We focus on the ω_c -dependence in $\tilde{G}_{i,i+L}(\tau)$ to study the limit $\omega_c \rightarrow \infty$. In (2.84), the relevant term is given by

$$e^{-\phi_0 L^2/2} = e^{-KL^2 \log(\beta\omega_c/2\pi)}.\quad (\text{D}\cdot 16)$$

Because the coefficient of L^2 includes ω_c , the Green's function $\tilde{G}_{i,i+L}(\tau)$ vanishes in the limit $\omega_c \rightarrow \infty$ for $L \neq 0$. To see a correct coefficient of L^2 , we must also consider the term $L^2 Q(n)$ in the exponent of (2.84). From (3.8), we obtain

$$Q(n) \simeq K \log(Kn)\quad (\text{D}\cdot 17)$$

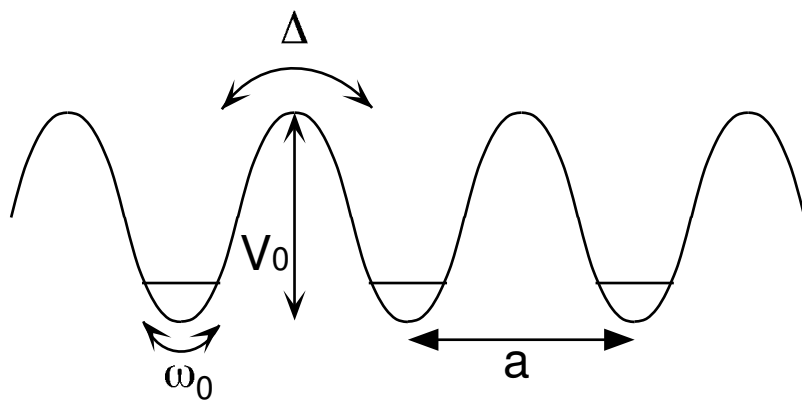
in the low-temperature limit $\beta \rightarrow \infty$ ($n \rightarrow \infty$). When we expand $Q(n(\theta))$ as $Q(\theta) \simeq Q(0) + Q''(0)\theta^2/2$, the coefficients satisfy $Q''(0) \ll U''(0)$ at low temperatures. Thus, we can neglect the correction $Q''(0)$ and the Green's function is calculated approximately as

$$\tilde{G}_{i,i+L}(\tau) \simeq -e^{-KL^2 \log(\beta\omega_c/2\pi Kn)}.\quad (\text{D}\cdot 18)$$

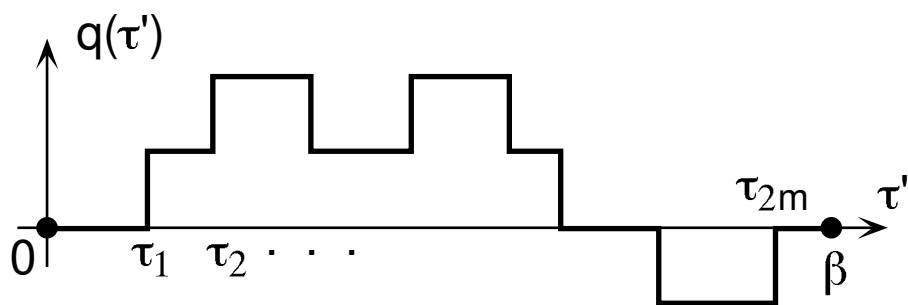
By using (D.8) and (3.23), we obtain (3.39).

- [1] U. Weiss: *Quantum Dissipative Systems* (World Scientific, Singapore, 1993).
- [2] J. Kondo: *Physica* **84B** (1976) 40.
- [3] J. Kondo: *Physica* **125B** (1984) 279.
- [4] K. Yamada: *Prog. Theor. Phys.* **72** (1984) 195.
- [5] R. Kadono, J. Imazato, T. Matsuzaki, K. Nishiyama, K. Nagamine, T. Yamazaki, D. Richter and J. -M. Welter: *Phys. Rev. B* **39** (1989) 23.
- [6] G. M. Luke, J. H. Brewer, S. R. Kreitzman, D. R. Noakes, M. Celio, R. Kadono and E. J. Ansoldo: *Phys. Rev. B* **43** (1991) 3284.
- [7] J. Kondo: *Prog. Theor. Phys.* **32** (1964) 37.
- [8] P. Nozières and C. T. de Dominicis: *Phys. Rev.* **178** (1969) 1097.
- [9] D. G. Clarke, S. P. Strong and P. W. Anderson: *Phys. Rev. Lett.* **74** (1995) 4499.
- [10] D. G. Clarke, S. P. Strong, P. M. Chaikin and E. I. Chashechkina: preprint (cond-mat, 9708081)
- [11] A. Barone and G. Paterno: *Physics and Applications of the Josephson Effect* (Wiley, New York, 1982)
- [12] I. L. Aleiner, N. S. Wingreen and Y. Meir: preprint (cond-mat, 9702001)
- [13] A. O. Caldeira and A. J. Leggett: *Ann. Phys. (N. Y.)* **149** (1983) 374; **153** (1984) 445(E).
- [14] A. J. Leggett, S. Chakravarty, A. T. Dorsey, M. P. A. Fisher, A. Garg and W. Zwerger: *Rev. Mod. Phys.* **59** (1987) 1; **67** (1995) 725(E).
- [15] M. P. A. Fisher and W. Zwerger: *Phys. Rev. B* **32** (1985) 6190.
- [16] W. Zwerger: *Phys. Rev. B* **35** (1987) 4737.
- [17] U. Eckern and F. Pelzer: *Europhys. Lett.* **3** (1987) 131.
- [18] Y. -C. Chen, J. L. Lebowitz and C. Liverani: *Phys. Rev. B* **40** (1989) 4664.
- [19] V. Hakim and V. Ambegaokar: *Phys. Rev. A* **32** (1985) 423.

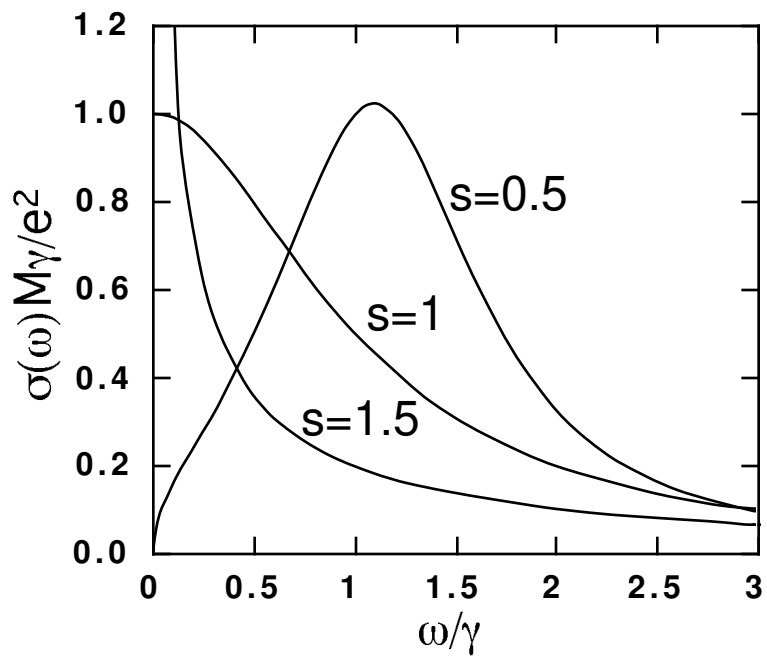
- [20] H. Grabert, P. Schramm and G. -L. Ingold: Phys. Rep. **168** (1988) 115.
- [21] U. Weiss and H. Grabert: Phys. Lett. **108A** (1985) 63.
- [22] U. Weiss and M. Wollensak: Phys. Rev. B **37** (1988) 2729.
- [23] M. Sassetti, M. Milch and U. Weiss: Phys. Rev. B **46** (1992) 4615.
- [24] A. Schmid: Phys. Rev. Lett. **51** (1983) 1506.
- [25] U. Weiss, M. Sassetti, T. Negele and M. Wollensak: Z. Phys. B **84** (1991) 471.
- [26] R. Görlich and U. Weiss: Phys. Rev. B **38** (1988) 5254.
- [27] F. Sols and F. Guinea: Phys. Rev. B **36** (1987) 7775.
- [28] R. P. Feynman: *Statistical Mechanics* (Benjamin, New York, 1972)
- [29] S. Chakravarty and S. Kivelson: Phys. Rev. B **32** (1985) 76.
- [30] A. T. Dorsey, M. P. A. Fisher and M. Wartak: Phys. Rev. A **33** (1986) 1117.
- [31] U. Weiss, H. Grabert, P. Hänggi and R. Riseborough: Phys. Rev. B **35** (1987) 9535.
- [32] C. G. Callan and S. Coleman: Phys. Rev. D **16** (1977) 1762.
- [33] S. Chakravarty: Phys. Rev. Lett. **49** (1982) 681.
- [34] A. J. Bray and M. A. Moore: Phys. Rev. Lett. **49** (1982) 1546.
- [35] R. Kubo: J. Phys. Soc. Jpn. **12** (1957) 570.
- [36] D. J. Scalapino, S. R. White and S. Zhang: Phys. Rev. B **47** (1993) 7995.
- [37] W. Kohn: Phys. Rev. **133** (1964) A171.
- [38] B. S. Shastry and B. Sutherland: Phys. Rev. Lett. **65** (1990) 243.
- [39] S. Chakravarty and J. Rudnick: Phys. Rev. Lett. **75** (1995) 501.
- [40] T. A. Costi and C. Kieffer: Phys. Rev. Lett. **76** (1996) 1683.
- [41] R. Egger, H. Grabert and U. Weiss: Phys. Rev. E **55** (1997) 3809.
- [42] For example, ref. 17 and ref. 22 fail in deriving the T^2 -suppression term.
- [43] W. F. Brinkman and T. M. Rice: Phys. Rev. B **2** (1978) 1324.
- [44] T. M. Rice and F. C. Zhang: Phys. Rev. B **39** (1989) 815.
- [45] W. Metzner, P. Schmit and D. Vollhardt: Phys. Rev. B **45** (1992) 2237.
- [46] J. E. Mayer and M. G. Mayer: *Statistical Mechanics* (John Wiley & Sons, 1940, New York)
- [47] L. D. Landau and E. M. Lifshitz: *Statistical Physics*, Part 1, 3rd. ed. (Pergamon Press, 1980, Oxford)

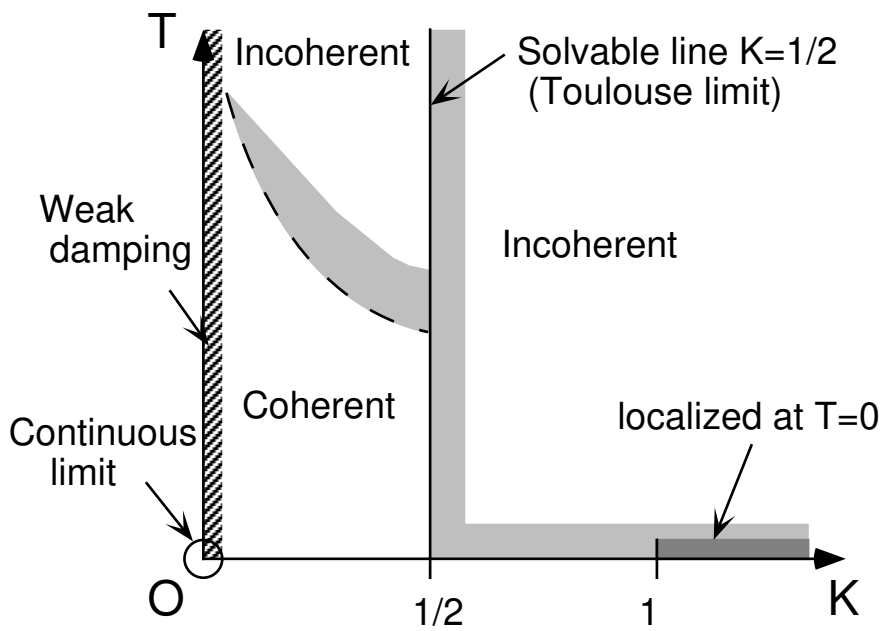


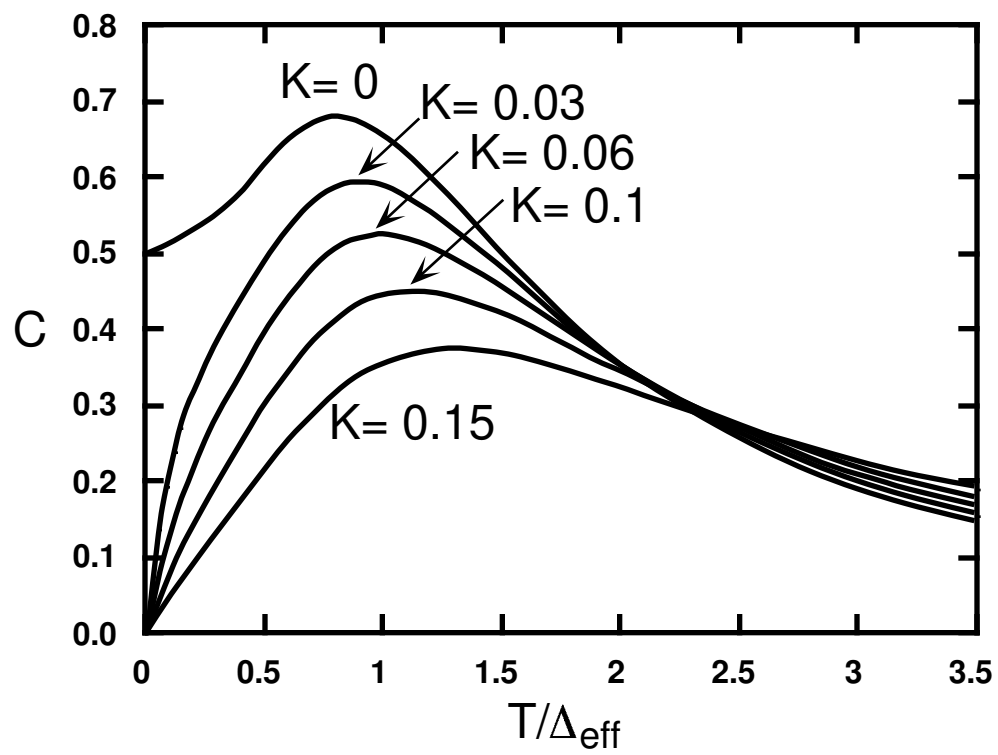
(a)

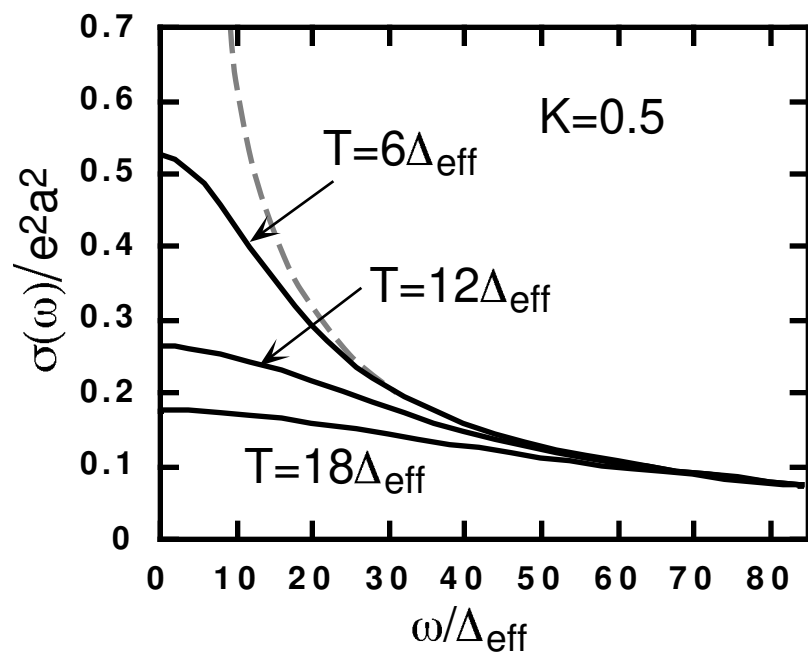


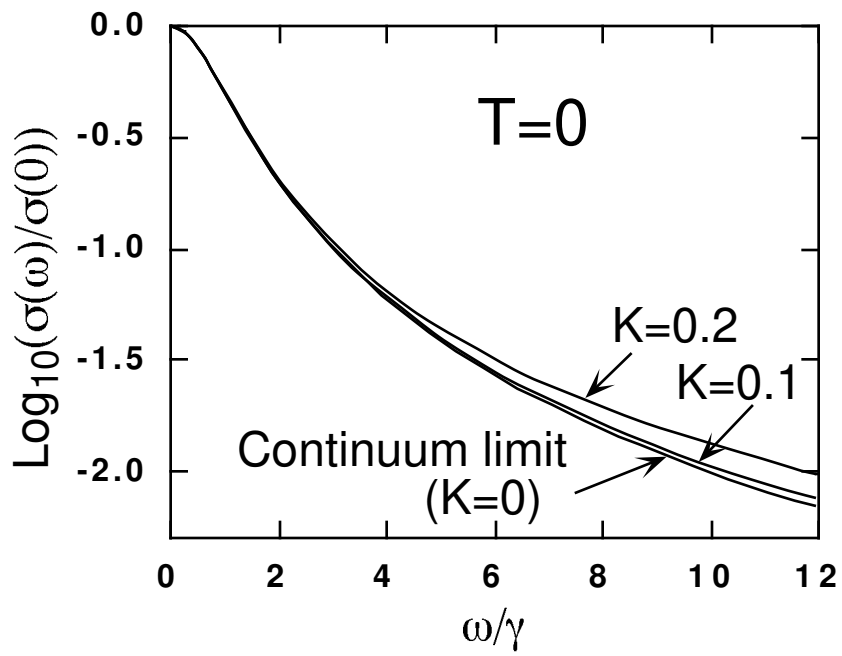
(b)











$$b_{2,0} = \frac{1}{2} \left[\begin{array}{c} \bullet \text{---} \bullet \\ 1 \qquad 2 \end{array} \right]$$

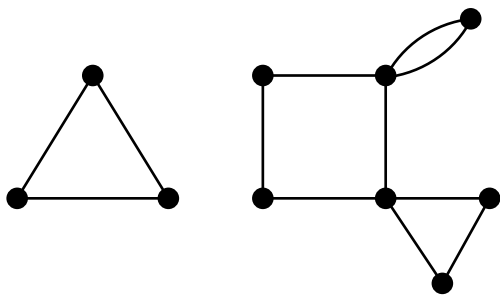
$$b_{1,1} = \left[\begin{array}{c} \bullet \text{---} \circ \\ 1 \qquad 2 \end{array} \right]$$

$$b_{3,0} = \frac{1}{6} \left[\begin{array}{c} \bullet \qquad \bullet \qquad \bullet \\ \diagup \quad \diagdown \\ \bullet \text{---} \bullet \\ 1 \qquad 2 \end{array} \quad + 3 \quad \begin{array}{c} \bullet \qquad \bullet \\ \diagdown \\ \bullet \text{---} \bullet \\ 1 \qquad 2 \end{array} \right]$$

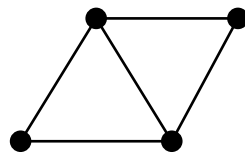
$$b_{2,1} = \frac{1}{2} \left[\begin{array}{c} \circ \qquad \bullet \qquad \bullet \\ \diagup \quad \diagdown \\ \bullet \text{---} \bullet \\ 1 \qquad 2 \end{array} \quad + 2 \quad \begin{array}{c} \circ \qquad \bullet \\ \diagdown \\ \bullet \text{---} \bullet \\ 1 \qquad 2 \end{array} \quad + \quad \begin{array}{c} \bullet \qquad \bullet \\ \diagdown \\ \bullet \text{---} \circ \\ 1 \qquad 3 \end{array} \right]$$

$$\begin{aligned}
 \text{thick line} &= \text{thin line} + \text{loop} + \text{double loop} + \dots \\
 \text{thick line with open circle} &= - \text{thin line} + \text{loop} - \text{double loop} + \dots
 \end{aligned}$$

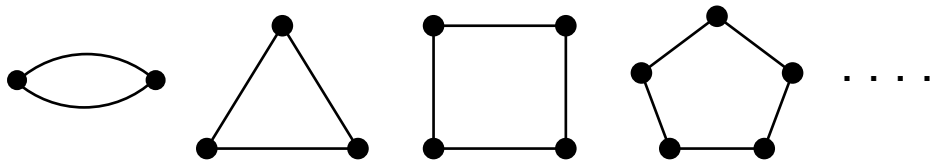
(a)



(b)



(c)



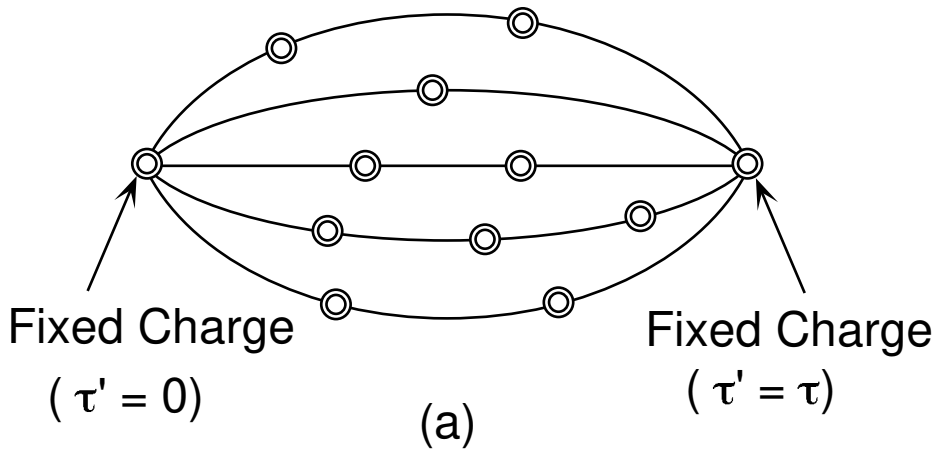


Diagram (b) shows a series expansion of a node. On the left, a node (circle) is connected to a line. This is equal to a sum of terms: a node connected to a line, plus a node connected to a line with a loop, plus a node connected to a line with two loops, plus an ellipsis. This is then simplified to a single term: a node connected to a line multiplied by α .

$$\text{Node} = \text{Node} + \text{Node} + \text{Node} + \dots$$

$$= \text{Node} \times \alpha$$

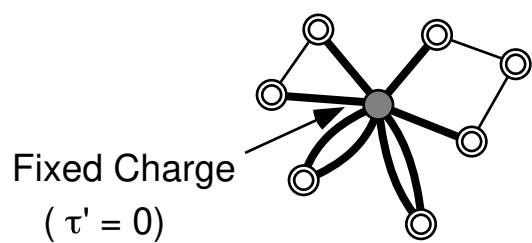
(b)

Diagram (c) shows a chain of nodes connected by a horizontal line. The chain is labeled C_1 and includes an ellipsis between the second and third nodes. A bracket underneath the chain is labeled "I-Charges".

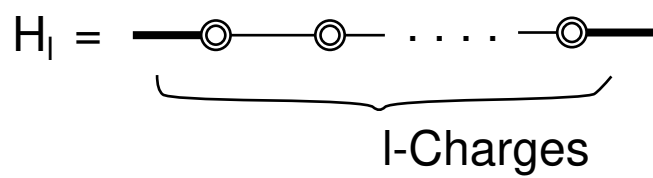
$$C_1 = \text{---} \text{---} \text{---} \dots \text{---}$$

I-Charges

(c)



(a)



(b)